INVESTIGATION OF THE EFFECT OF TEMPERATURE ON FRACTURE BEHAVIOUR OF WELDED API X70 STEEL

BY

EGENE, Matthew Simon

(M.ENG/SEET/2017/6972)

DEPARTMENT OF MECHANICAL ENGINEERING

FEDERAL UNIVERSITY OF TECHNOLOGY,

MINNA

NOVEMBER, 2021

INVESTIGATION OF THE EFFECT OF TEMPERATURE ON FRACTURE BEHAVIOUR OF WELDED API X70 STEEL

BY

EGENE Matthew Simon

(M.ENG/SEET/2017/6972)

A THESIS SUBMITED TO THE POSTGRADUATE SCHOOL FEDERAL UNIVERSITY OF TECHNOLOGY, MINNA, NIGERIA IN PARTIAL FULFILLMENT OF THE REQUIREMENTS FOR AWARD OF MASTER OF ENGINEERING (M.Eng) IN MECHANICAL ENGINEERING (INDUSTRIAL AND PRODUCTION ENGINEERING OPTION)

NOVEMBER, 2021

ABSTRACT

Oil and gas production has significantly increased over the years in order to meet present demands for oil and gas products, regardless of the unstable price being experienced by producing Nations. The use of pipelines for the transportation of these products has been the globally recognized solution. These pipelines are fabricated by welding and their fracture properties depend on a number of factors which include temperature, particularly for the pipelines operating in cold region such as deeper water depths. Therefore, information of fracture behavior of welded pipelines located in cold regions is therefore important for reliable design service. In this work, the effect of temperature on fracture behavior of welded API X70 steel was investigated using Charpy V- notch specimens. The scanning electron microscope (SEM) and spectroscosopic analyses were carried out on the fractured surfaces of parent and weld specimens. Impact tests were carried out on weld and parents at temperatures -10^0C, -20^0C, -40^0C, -60^0C, -80^0C, -100^0C, -120^0C, -160^0C, 0^0C, 10^0C and 20^0C. Results reveal that higher energy was absorbed in the weld than in parent materials regardless of the test temperature used. The Charpy energy dropped from 145.6 J to 12.3 J as the test temperature were reduced from 20^0C to -160^0Cwhich implies that energy absorbed during charpy test is sensitive to temperature. The tensile properties of parent and weld materials were determined at room temperature. The mean yield and strength as well as the mean yield /tensile ratio of the parent materials were determined to be 561.05Mpa, 632.50Mpa and 0.89 respectively. Meanwhile, the mean yield and strength and the mean yield/tensile ratio of the weld materials were determined to be 575.69Mpa, 668.61Mpa and 0.86 respectively

TABLE OF CONTENTS

Content	Page
Title Page	ii
Declaration	iii
Certification	iv
Dedication	v
Acknowledge	vi
Abstract	vii
Table of Content	viii
List of Tables	xi
List of Figures	xii
List of Plates	xiv
Abbreviations, Symbols and Units	xv
CHAPTER ONE	
1.0 INTRODUCTION	1
1.1 Background of the Study	1

1.2 Statement of Research Problem 2

1.3 Justification of the Research 3

1.4 Aim and Objectives of the Research 3

1.5 Scope of the Research 3

CHAPTER TWO

2.0 LITERATURE REVIEW 4

2.1 Introduction 4

2.2 Pipeline Steel Grades 4

2.3 Pipeline Welding 8

2.4 Fracture Assessment of Steel Materials 10

2.5 Fracture Toughness of Pipeline Steels 12

2.5.1 Fracture toughness correlations using Charpy V-notch specimens 15

2.6 Review of Fracture Behaviour and Mechanical Characterization of API Steel Grades 18

2.7 Factors Affecting the Fracture Properties of Pipeline Steels 24

2.7.1 Stress concentration 24

2.7.2 Material modification by welding, peeling and rolling 27

2.7.3 Temperature effect 29

2.7.4 Effect of test environment 30

2.7.5 Welding and residual stress 32

2.7.6 Research Gap 35

CHAPTER THREE

3.0 MATERIALS AND METHODS 36

3.1 Materials 36

3.2 Methods 39

3.2.1 Chemical analysis of the material by spectroscopic method 39

3.2.2 Welding and Specimens preparation 39

3.3 Charpy Specimens Extraction and Testing 40

3.3.1 Tensile Specimens and Extraction and Testing 42

3.3.2 Fracture toughness calculation using Charpy V-notch correlations 44

CHAPTER FOUR

4.0 RESULTS AND DISCUSSION 46

4.1 Spectroscopic Analysis of Results 46

4.2 Charpy V-notch test Results and Discussion 47

4.3 Tensile test Results and Discussion 54

4.4 Fracture Toughness Results and Discussion 56

CHAPTER FIVE

5.0 CONCLUSIONS AND RECOMMENDATIONS 61

5.1 Conclusions 61

5.2 Recommendations 62

5.3 Contribution to Knowledge 62

REFERENCES 64

APPENDICES 67

LIST OF TABLES

Table	Title	Page
2.1	Chemical composition of X80 pipeline Steel	7
2.2	Chemical composition of sample API X70 Steel	7
2.3	Summary of pipeline failure with their causes and locations	33
3.1	Equipment	36
4.1	Chemical composition of API X70 steel	46
4.2	Chemical composition of API X70 steel	46
4.3	Tensile properties of base material	55
4.4	Tensile properties of weld material	56

LIST OF FIGURES

Figures	Title	Page
2.1	Material composition variations for API steel grades	5
2.2	Schematic diagram of submerged-arc welding process	9
2.3	Different types of weld joint	10
2.4	Charpy curve showing ductile- brittle transition temperature	13
2.5	Charpy V-notch curve for a 0.06C 0.5Ni steel weld metal	14
2.6	Microstructure of (a) API X70 (b) API X80 (c) API X100 steels	19
2.7	Fracture behaviour of pipe with (a) lower corrosion rates (b) Higher corrosion rates	21
2.8	Charpy impact energy versus temperature	23
2.9	Stress distribution in (a) plate with a center hole under tensile load (b) Plate notched at both sides under load	26
2.10	Shot peening processes	28
2.11	Longitudinal residual stresses in a butt weld	34
2.12	Pattern of residual and applied stresses	35
3.1	Weld plate edge preparation	40

3.2	Charpy V-notch specimens extraction	40
3.3	Charpy V-notch geometry	41
3.4	Weld tensile test specimen design	44
4.1	Charpy V-notch energy absorbed in parent materials	48
4.2	Charpy V-notch energy absorbed in weld materials	49
4.3	Comparison of Charpy energy absorbed in parent and weld materials	51
4.4	SEM analysis of (a) parents specimens (b) weld specimens	53
4.5	Fracture toughness- Charpy energy correlation for parent material	57
4.6	Fracture toughness- Charpy energy correlation for weld material	59

LIST OF PLATES

Plate	Title	Page
I	UNITED type universal testing machine	37
II	Charpy V-notch impact testing machine	38
III	Blacks Charpy V-notch machine	38
IV	Extracted Charpy V-notch specimens from Parent plate and weld area	41
V	Parent tensile test specimens	43
VI	Weld tensile test specimens	43
VII	Fracture Surfaces of (a) Parent Specimens (b) Weld Specimens	52

ABBREVIATIONS, SYMBOLS AND UNITS

Notation	Acronyms	Units
American petroleum institute	API	-
Heat Affected Zone	HAZ	-
Carbon Equivalent	CE	-
Drop weight tear test	DNTT	-
Mammal metal Arc welding	MMA	-
High strength low Alloy steels	HSLA	-
British standard	BS	-
Charpy V-Notch	CVN	-
Vickers hardness number	HV	-
Scanning Electron microscope	SEM	-
Transmission Electron microscope	TEM	-
Post weld heat treatment	PWHT	-
American standard for testing materials	ASTM	-

CHAPTER ONE

1.0 INTRODUCTION

1.1 Background of the Study

Oil and gas production has significantly increased over the years and in order to meet present demands for oil and gas products, the use of pipelines for the transportation of these products has been the globally recognized solution. The significant demand for oil and gas products necessitate the transportation of the products over a long distance to where they are demanded (Wang *et al.*, 2014). These pipelines are made of different steel grade and the choice of a particular grade for specific purpose depends on the area of application, environment and required operating pressure, to mention but a few (Vegas, 2014). However, pipelines are manufactured according to the requirements in the API 5L standard. Pipelines are fabricated by welded sections. They are mostly subjected to internal loading due to the pressure for the transportation medium as well as external loading particularly for pipelines that are installed in dynamic environments. During service, due to the nature of stress concentration, cracks can initiate in welded areas which are potential spots for crack initiation and subsequent propagation to sudden failure or collapse. As such, a better understanding of the fracture toughness of pipeline is necessary in order to provide useful information to design Engineer regarding inspection, prediction or estimation of the service lives of pipelines in service.

Pipeline steel grade that are commonly used are those that are specified as API X52, X60, X65, X70, X80 and X100 (Vegas, 2014). It must be mentioned that most pipeline installation in Nigeria are made of the X55 and X60 grades which are lower in toughness compared to the recent grade such as X70, X80 and X100. It was mentioned that the earlier fabricated pipeline steels are the C-Mn steels such as X42 and X52 grades, which contain higher carbon content compared to the newer grade of pipeline steels (X70, X80 and X100) (Vesga, 2014). The carbon content of these steels is reduced in order to improve weldability, mechanical strength and fracture properties. Fracture properties of steels depend on a number of factors which include temperature particularly for pipelines operating in cold environment such as deeper water depths. Under dynamic loads, crack initiates from the weld heat affected zone (HAZ) and propagate into the parent material (Adedipe *et al.,* 2015). The weld HAZ is part of the parent or base materials but it is characterised by a different microstructure due to the type of welding, filler material, plate thickness. Failure or crack propagation of API steels grades may be different under a low temperature due to environmental influence. It is therefore important to have better understanding of the fracture properties of these steels under a low temperature for estimating of their lives in service. In this research, the fracture properties of API X70 steel was investigated. Tests were conducted on charpy V-notch specimens subjected to cold environment.

1.2 Statement of Research Problem

Quite a number of API steel grades have been installed to transport oil and gas products. Most of the pipelines installed in Nigeria are the API X55 and X65 steel grades. In the future, an update to the Nigeria pipeline networks may be needed. The most commonly

used pipeline globally is the API X70 steel due to its cost. The fracture behaviour of pipeline steels depends on the type of steel material, the nature of operating environment as well as the type of loading which the materials experience in service. The range of temperature especially for pipelines that are installed in marine environments could be site dependent.

1.3 Justification of the Research

For better understanding of the behaviour of API X 70 steel, there is therefore a need to investigate the effect of temperature on the fracture property of API X70 steel. As such, information regarding fracture toughness may assist design Engineers in structural health monitoring, maintenance planning and replacement of structures if necessary.

1.4 Aim and Objective of the Research

The aim of this research is to investigate the effect of temperature on fracture behaviour of API X70 steel modified by welding. Sequel to the aim, the objectives are:

1. To determine the chemical composition of the API X70 steel
2. To carry out impact tests on charpy V-notch parent and weld specimens extracted from the X70 steel at various temperatures
3. To carry out tensile tests on the parent and weld materials at room temperature
4. To determine the fracture toughness of the API X70 steel using charpy V-notch correlations and
5. Determination of microstructural examination.

1.5 Scope of the Research

Only API X70 steel was used for investigations in this research. Charpy V-notch specimens were extracted from the steel plate and impact tests were carried out on them at different

temperatures. Estimation of fracture toughness using correlations was limited to the use of the results obtained from impact energies absorbed by the specimens. Tests were also supported by spectroscopic analysis and tensile property of the material.

CHAPTER TWO

2.0 LITERATURE REVIEW

2.1 Introduction

In this chapter, a review is presented to address the factors that influence the fracture behaviour of pipeline steels grades. There are so many factors responsible for the fracture behaviour of steels generally. However, experimental investigations considering all the factors may be time consuming. This is probably why most investigations consider a few. However, relevant review and information about the factors are important for better understanding of their interaction. A review of pipeline steel grades is first presented in the next section.

2.2 Pipeline Steel Grades

There are different pipeline steel grades but the earlier reported ones in the literature are the C-Mn steels of X42 and X52 which have been mentioned to have poor toughness due to the composition of carbon (Vesga, 2014). One of the ways to characterize steels generally is by the amount of carbon. To obtain better toughness, weldability and strength, steel producers now use improved manufacturing techniques coupled with reduction in carbon contents. Some of the alloying elements that are added to these steels to obtained the needed strengths include aluminium, vanadium, niobium and titanium (Adegbite, 2014). The

manufacturing trend through the addition of carbon and some other elements (V, Nb, Ti, B) for pipeline steels produced from 1965 to 2008 is shown in Figure 2.1.

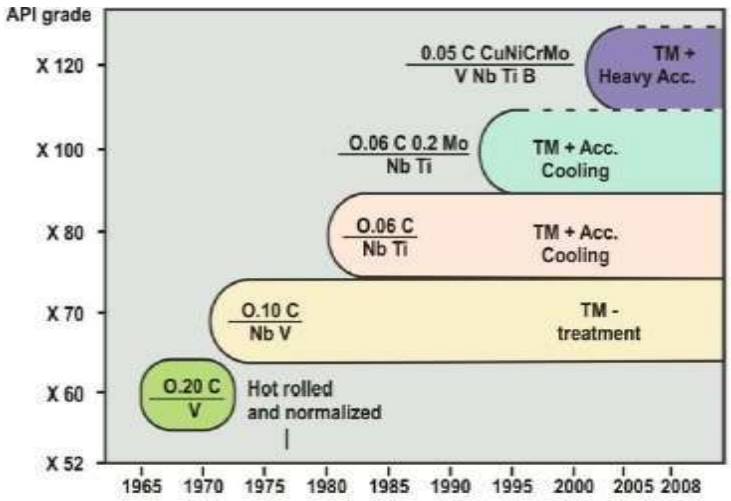

Figure 2.1: Material composition variation for API steel grades (Hillenbrand *et al.*, 1999)

From Figure 2.1, it can be seen that the carbon content of the steels is reduced as the grades are modified over the years. Around the year 1960, there was brittle fracture in a gas pipeline in United States of America (USA) and this led to the use of Battelle drop weight tear test (DWTT) as a requirement for fracture assessment of pipeline steels; and this is one of the factors that informed the change in steel making process (Mustapha, 2010). In the literature, some of the investigation on pipeline steels materials considering properties such as weldability, toughness and strength are those reported in (Hillenbrand *et al.*, 1999; Liessem and Hillenbrand, 2007; Hillenbrand *et al.*, 2008). Summarily, the investigations that were carried out involved the selection of the optimum rolling condition, chemical composition and cooling rate (Vesga, 2014).

Hillenbrand *et al.* (1999) established that pipeline materials are being used due to peculiar nature of mixed phase microstructures coupled with fine grain. It was also mentioned that the highest grade of pipeline steel that can be manufactured with pearlite-ferrite microstructure while retaining the weldability as well as ductile-brittle transition temperature is the X70 steel grade (Hillenbrand *et al.*, 1999). However, it could be said that the quest for better manufacturing techniques that will enhance toughness and other related mechanical properties therefore informed the recent use of high strength low alloy steels (HSLA), which include X52, X60, X65, X70, X80, X100 and X120 (Vesga, 2014). Their reliable mechanical properties may be a factor that justifies their usage for structural applications as well as in the transportation of oil and gas products.

However, due to cost implication and the specific need for area of application, the most commonly used pipeline steels are the API X80 and X70 grades. API X70 steels are used in oil and gas pipelines, shipping industries, oil storage tanks and temporal bridges for road construction (Ike, 2018). A typical composition of API X80 steel is shown in Table 2.1, while Table 2.2 shows the chemical composition of X70 steel. However, a confirmatory test was carried out on the API X70 steel that was used for investigation in the present research. The result is discussed in chapter 4.

Table 2.1 Chemical composition of X80 pipeline steel (Wang *et al*., 2014)

Steel	C	Si	Mn	P	S	Ni	Mo	u	V	Al	Nb	Ti	Fe	
X80	0.07	0.30	1.77	0.02	0.005	0.22	0.21	0.22	0.06	0.06	0.05	0.021		bal.

Table 2.2. Chemical compositions of sample API X70 Steel (Ike., 2018)

Elements	%C	%Fe	%Si	%Mn	%Cr	%Mo	%Ni	%V	%Cu	%Al	CE(IIW)
Base metal	0.051	97.73	0.210	1.510.	0.240	0.118	0.071	0.021	<0.002	0.048	0.38

Pipelines generally must exhibit some important properties in order to maintain their integrity during their service lives. These properties are strength, toughness and weldability. Strength is the ability of a welded pipeline to withstand all the dynamic or operational forces acting upon it. The strength of steels can be increased by addition of alloying elements such as C, Si and Mn, grain refinement as well as strengthening through the formation of martensite and bainite (Mustapha., 2010). Toughness on the other hand is the ability of a pipeline to withstand crack propagation and fracture. Apart from stress raisers or concentrations, these cracks can originate in pipeline due to its contact with the environment or from third party events such as pipeline transportation, installation and activities from vandals. Weldability is the ability of steel to respond effectively to welding without cracking or increased hardness (Mustapha., 2010). This is one of the reasons why steel manufacturers reduce carbon contents as weldability of steels is controlled by the

carbon content. It was mentioned that as carbon content in steel is increased, the tensile strength and carbon equivalent are enhanced; as such, an increase in carbon equivalent would lead to decrease in weldability (Mustapha., 2010).

2.3 Pipeline Welding

Welding is a process which involves the joining of two similar or dissimilar metals by heating to appropriate temperature with or without pressure and with or without the use of filler material (Palmer and King, 2004). Pipelines are generally made of welded sections and the process involved adequate control of heat input, heat input rate and protection of the molten material from oxidation during welding. Transportation of oil and gas products often requires a continuous process that can only be achieved through the use of pipelines. Due to the nature of loading scenarios from the transporting fluids, environmental conditions as well as externally applied dynamic loads that pipelines experience in service, appropriate welding techniques are therefore needed for their fabrication. Requirements such as chemical compositions, mechanical properties and different manufacturing techniques that are particular to oil and gas pipelines are set out according to the specifications of the American Petroleum Institute (API). Welding causes thermal and microstructure changes in pipeline steels, therefore the choice of the consumables that are used for welding should be taking into consideration before estimating the behaviour of the material (API Energy 2008). Pipeline steel grades can be fabricated by either welded or seamless; the latter process being an hot working process that is used to manufacture tubular sections without a welded seam (Sharma and Maheshwari, 2017).

API pipeline welding techniques used has been categorized into two processes. First, welding process in the absence of filler material which are continuous welding, electric welding and laser welding; and second, welding process with the use of filler material (submerged-arc welding (SAW), gas metal-arc welding (Sharma and Maheshwari, 2017). The submerged-arc welding process is one of the recognized techniques for the manufacture of longitudinal and circumferential butt weld that are required for the fabrication of pipelines and pressure vessels. The filler material may be a solid or coiled wire that is operated by a mechanical process and with the application of welding current of between 300 to 1000 Amperes. During the SAW process, an arc is formed between the filler material that is continuously fed and the work piece. A protective layer of gas shield and slag are formed in the process to protect the weld zone. The schematic diagram of submerged-arc welding process is shown in Figure 2.2.

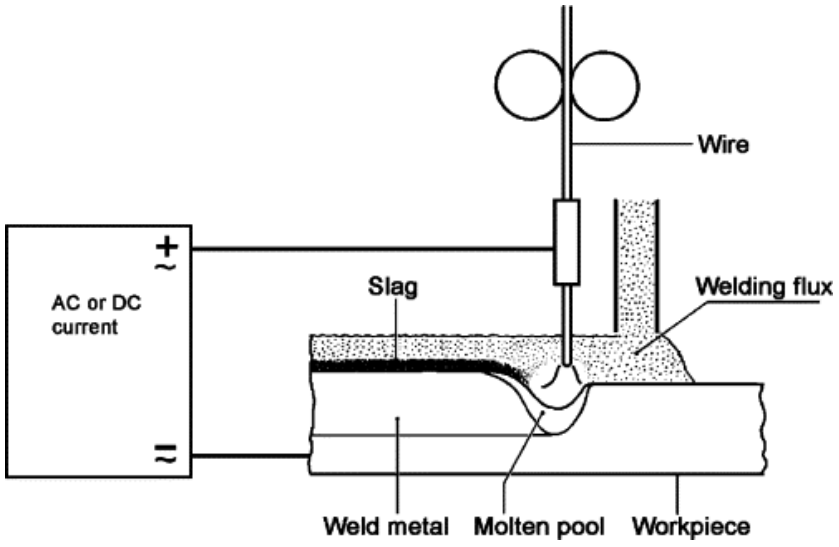

Figure 2.2: Schematic diagram of submerged-arc welding process (Naidu *et al.*, 2003)

There are different types of weld joints. These are square butt preparation, single V, double V and single U preparations, T-joint, Lap-joint assembly and T-joint with single J-preparation (Weman, 2003). A schematic representation of these can be seen in Figure 2.3. However, a choice of particular joint for specific purpose may depend on the area of application, material type, material thickness, type of welding process and the nature of load on the material.

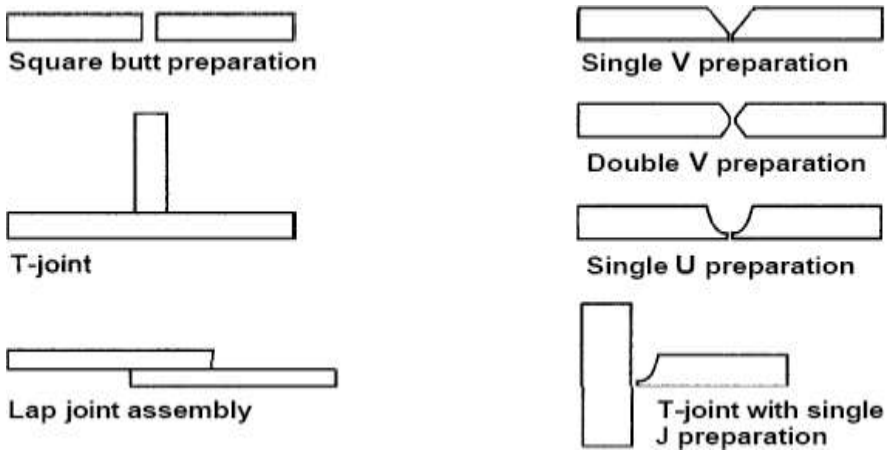

Figure 2.3: Different types of weld joint (Weman, 2003)

2.4 Fracture Assessment of Steel Materials

Lifetime assessment in structures and components with respect to crack propagation is studied by fracture mechanics. Fracture in materials can be studied by two methods; energy criterion and stress intensity factor approach (Anderson, 2005). The energy based criterion which is proposed by Griffith (Griffith, 1920), states that the growth of crack would occur in a materials if the energy that is available to cause crack propagation is adequate to overcome the strength of the material (Anderson, 2005). The Griffith criterion is expressed in Equation 2.1 for an infinite plate with crack length $2a$ subjected to tensile stress σ.

$$\frac{dU}{da} = \frac{dW}{da} \tag{2.1}$$

Where U is the released energy and W is the energy required to cause crack growth. Griffith determined $\frac{dU}{da}$ for an elliptical crack (Inglis, 1913) as:

$$\frac{dU}{da} = \frac{2\pi\sigma^2 a}{E^*} \tag{2.2}$$

$E^* = E$ for plane stress cases and $E^* = \frac{E}{(1-\nu^2)}$ for plane strain cases, E = Young's modulus, ν = Poisson's ratio. If the left of Equation 2.2 is replaced by a factor G known as strain energy in the material that is enough to effect crack growth, the equation becomes

$$G = \frac{\pi\sigma^2 a}{E^*} \tag{2.3}$$

Where a is half of crack length under consideration. During fracture, under critical stress σ_c, the factor G in Equation 2.3 becomes G_{Ic} which is expressed as:

$$G_{Ic} = \frac{\pi\sigma_c^2 a}{E^*} \tag{2.4}$$

G_{Ic} is critical energy release rate. The critical stress at fracture can then be determined by (Inglis, 1913)

$$\sigma_c = \sqrt{\frac{E^* G_{Ic}}{\pi a}} \tag{2.5}$$

Strain energy release rate G and fracture toughness K with respect to the energy criterion can also been expressed as (Beden *et al*., 2009)

$$G = \frac{K^2}{E^*} \tag{2.6}$$

Equations 2.2 to 2.6 are used for energy-based criterion for fracture assessment. The other method which is the stress intensity approach can be found in (Anderson 2005). However, stress intensity approach can only be used for crack propagation test data, which was not considered in the present study.

2.5 Fracture Toughness of Pipeline Steels

Due to industrialization, significant drilling of oil globally and reduction in quantity of natural gases, drilling in the cold reservoirs are being required (Shin *et al.*, 2009). Fracture assessment of pipelines operating in cold region has therefore become important so that design, inspection and structural health monitoring Engineers can make reliable estimation of evaluation of service lives of these pipelines. Fracture in pipelines is dominated by crack initiation and propagation. However, ductile and brittle fractures are the two most common failure mechanisms in pipelines. These mechanisms are associated with structural integrity or toughness at low temperature; and are described by ductile brittle transition temperature (DBTT). DBTT is the minimum temperature at which a specific material is able to absorb a particular amount of energy without fracture (―www.spartaengineering.com‖ 2020). The temperature is determined conventionally by breaking a notched bar using impact tester and by measuring the energy absorbed during fracture (Lancaster, 2005). Experimental investigations are therefore necessary to for the assessment of pipelines that are exposed to cold environments. Impact tests are carried out at different temperatures, the values of the absorbed energy are plotted against the temperatures and the shape of the curve gives an S-shaped as shown in Figure 2.4 also The DBTT can be seen as the dotted lines. Figure 2.5

shows the typical Charpy V-notch curve for a 0.06C 0.5Ni steel weld metal (Lancaster, 2005). The explanation of these curves is that some materials which are ductile at room temperatures are brittle at low temperatures. This suggests that it is necessary to estimate the temperature at which the absorbed energy in a material becomes minimum. However, this temperature may be material dependent.

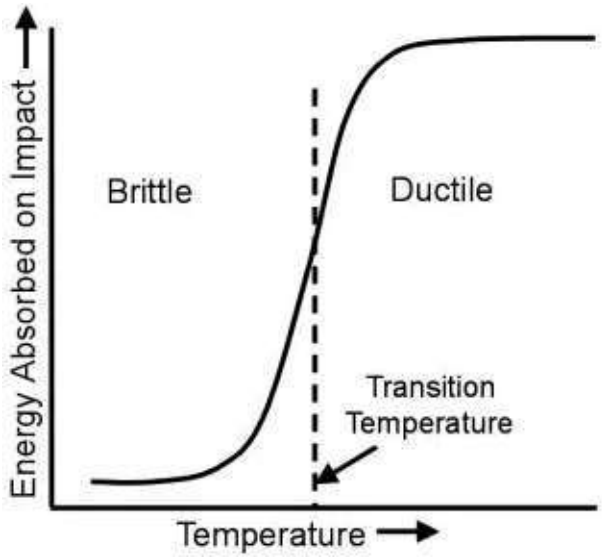

Figure 2.4: Charpy curve showing ductile-brittle transition temperature (Source: –www.quora.com‖ 2020)

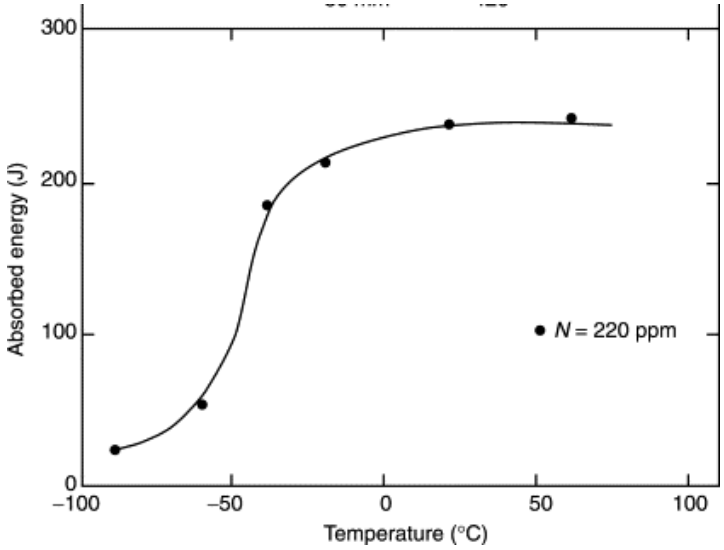
300
200
100
0
Absorbed energy (J)
−100
−50
0
50
100
Temperature (°C)
N = 220 ppm

Figure 2.5: Charpy V-notch curve for a 0.06C 0.5Ni steel weld metal (Source: Lancaster 2005)

The most commonly used tests for the determination of energy absorbed in a material is the Charpy impact test and the drop-weight test tear test (Mannucci and Harris 2002; Vesga Rivera 2014). When charpy tests are carried out either on precracked or notched charpy test specimens, the energy absorbed are plotted with respect to temperature. Generally, from the graph, the variation of absorbed energy versus temperature can be divided into three different regions as shown in Figure 2.4. These regions are lower shelf, intermediate zone and upper shelf. Lower shelf is associated with brittle fracture, while the upper shelve is associated with ductile fracture.

2.5.1 Fracture toughness correlations using charpy v-notch specimens

Fracture toughness (K_{IC}) is a material property; hence, determination of fracture toughness of a material depends on a number of factors which are discussed in a later section. However, one of the major factors influencing the fracture toughness is material thickness. Toughness is a property that plays significant role in evaluating the integrity coupled with monitoring of engineering structures such as pipelines, pressure vessels, automobiles, aircrafts and offshore structures. The usual practice for the determination of fracture toughness as explained in (BS 7910 2013) is to use the adequate thicknesses that are representative of the structure or component under consideration. But because of cost implication and the limitation of test machines that could accommodate thicker specimens, thinner materials have been suggested as alternatives. When a valid thickness that is representative of the real structure under consideration cannot be used to determine fracture toughness, (BS 7910, 2013) suggested that literature materials can be used as long as they

are similar to the structure being assessed. Another possible alternative that was suggested (BS 7910, 2013) is to obtain charpy notch data and determine fracture toughness values using correlations from the literature. Although, direct measurement of fracture toughness data may be preferable, but in situations where such data do not exist, charpy V-notch data are obtained from material of similar microstructure (Weld, HAZ and parent material), to obtain an estimated fracture toughness $K_{mat.}$ using the correlations have been described in (BS 7910 2013). A correlation for lower shelf and transition behaviour for charpy energy obtained at a single temperature is described as (BS 7910, 2013)

$$K_{mat} = [(12\sqrt{C_v} - 20)\left(\frac{25}{B}\right)^{0.25}] + 20 \qquad (2.7)$$

Where:

K_{mat} = the estimated fracture toughness ($MPa\sqrt{m}$)

B = thickness of the material (mm)

C_v = lower bound Charpy V-notch impact energy at the service temperature (J)

Other lower shelf or lower transition temperature correlations have also been developed to estimate fracture toughness of materials. The ones developed for lower shelf and transition temperature are given by (Barson and Rolfe, 1970).,

$$K_{IC}^2 = 45.1 * CVN^{1.5}$$

$$K_{IC}^2 = 105 * CVN$$

K_{IC} = fracture toughness of the material ($MPa\sqrt{m}$)

CVN = Charpy v-notch energy (J).

Equation 2.8 was for material with ultimate tensile strength range 270 to 1700 MPa, *CVN* range 4 to 82J and temperature range -196 to 27°C. Similarly, Equation 2.9 was developed for material with ultimate tensile strength range 270 to 1700 MPa, *CVN* range 3 to 61J and temperature range -196 to 0°C. A correlation developed by Sailors and Corten (1972) for lower shelf is expressed as:

$$K_{IC} = 14.6 * (CVN)^{0.5} \quad (2.10)$$

(Sailors and Corten, 1972) correlation was developed for material with ultimate tensile strength range 410 to 815 MPa, *CVN* range 7 to 70J. (Marandet and Sanz 1977) developed another correlation to estimate fracture toughness of material ultimate tensile strength range 274 to 820 MPa, *CVN* range 5 to 50J and temperature range -196 to 50°C. The correlation is expressed as:

$$K_{IC} = 19 * (CVN)^{0.5} \quad (2.11)$$

(Roberts and Newton 1984) developed a correlation for lower shelf region expressed as:

$$K_{IC} = 8.47 * (CVN)^{0.63} \quad (2.12)$$

The upper shelf correlation that are developed with respect to the yield strength of the materials are those developed by Barsom and Rolfe (1999) and Roberts and Newton (1984). The correlations are expressed in Equations 2.13 and 2.14 respectively.

$$\left(\frac{K_{IC}}{\sigma_{ys}}\right)^{2} = 0.64 * \left(\frac{CVN}{\sigma_{ys}} - 0.01\right) \quad (2.13)$$

$$K_{IC} = 0.804\sigma_{ys} * \left(\frac{CVN}{\sigma_{ys}} - 0.098\right)^{0.5} \quad (2.14)$$

Where σ_{ys} = yield stress of the material (MPa). Equation 2.13 was developed for material with yield stress in the range of 170 to 760MPa. It was mentioned that the correlations that

were developed by Barsom and Rolfe (1970), Sailors and Corten (1972), Marandet and Sanz (1977) have been considered for use significantly in the literature for estimating fracture toughness of materials form Charpy V-notch energy values. The only one among these correlations that consider material or specimen thickness regardless of temperature is the one that was developed by Marandet and Sanz (1977).

2.6 Review of Fracture Behaviour and Mechanical Characterisation of API Steel Grades

Mechanical characterizations refer to some of the investigations that have been carried out regarding the microstructure and mechanical properties of API pipeline steel grades. Due to materials variability enhanced by microstructure, material property as well as manufacturin g procedure such as welding, it is expected that the mechanical properties of pipeline steel grades will vary. In a study conducted by Cheng and Xue (2011), microstructure and mechanical properties of X70 and X80 pipeline steels were investigated. Microstructure investigated was conducted using scanning electron microscope (SEM) and transmission electron microscope (TEM). The mechanical properties that were investigated include tensile test and fracture toughness test using charpy samples. It was found that the effect of material variation influenced the mechanical properties of the two steels. However, the only set back in the investigation was that the effect of temperature on the fracture properties of the material were not adequately investigated. As such, it must be mentioned that transition behaviour regarding fracture properties of steels generally is temperature dependent. The investigation carried out on the similar pipeline laid in the 1980s by Aliu (2012) revealed that the pipelines belong to the class of High Strength Low Alloy Steel. In the work Aliu

(2012), the tests that were carried out include charpy and tensile tests. Fracture properties of the steel material were not estimated.

Godefroid *et al*., (2014) compared the microstructure and mechanical properties of X60 and X70 base steel materials. It was found that X70 steel has lower carbon content as well as better mechanical properties in terms of tensile, impact and hardness tests. The better results gotten from API X70 steel may be explained in the grain refinements by the addition of other elements coupled with the reduction of carbon content and the enhancement of strength. The mechanical properties, microstructure and toughness of X70 pipeline steel was investigated by Muneer et al. (2015). It was found that the steel exhibited better mechanical and fracture properties when compared with lower pipeline steel grades. Microstructure and mechanical properties of API X100 steel that is strengthened with copper (Cu) which had control on the fatigue crack growth mechanism as well as material ductile fracture behaviour Wallin *et al*. (2004). The effect of copper significantly enhanced the strength and toughness. Microstructures of some of the API steel grades have been investigated and it was found that X70 is ferrite-pearlite matrix, X80 is ferrite-bainite while X100 correpsonds to the bainite microstructure. A typical microstructure of the steels is shown in Figure 2.6.

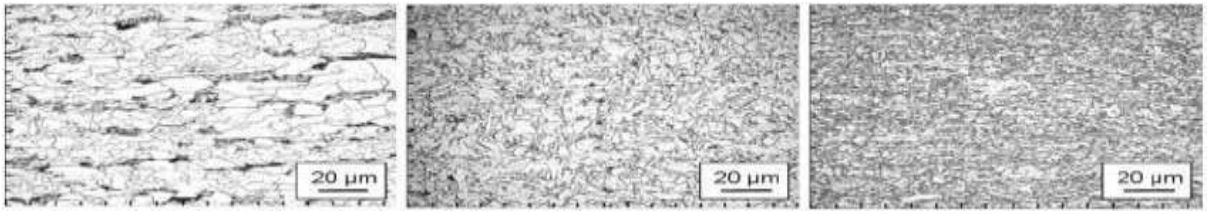

(a) (b) (c)

Figure 2.6: Microstructure of (a) API X70 (b) API X80 (c) API X100 steels (Hillenbrand *et al.,* 2008)

Mechanical and microstructure properties of weld pipeline steel were investigated by (Omale 2016). Microstructure investigation using optical microscope and TEM revealed that the base material of the X70 steel has equiax ferrite grains while the microstructure of the welded joint revealed acicular ferrite and fine bainite grains. Hardness value ranged from the weld joint to the parent and to the heat affected zone (HAZ) in descending order. However, charpy tests were not considered with respect to temperature. A similar result in terms of types of grains found in API X70 steel was revealed in an investigation conducted by (Omale *et al*., 2017). Most of the results published in the aforementioned literatures have not investigated the fracture properties of API X70 steel either experimentally or by using the available fracture toughness-charpy energy correlations that are available in the literature. As mentioned earlier, most of the Nigeria pipeline steels were laid in the 1980s and it should be mentioned that some of these pipelines may have exceeded their design lives even if they are still operational. Further investigations are therefore needed.

Nature of operating environment is another factor influencing the failure mechanisms and mechanical properties of pipeline steels. The influence of H_2S environment on tensile and fracture properties of API X70 steel was investigated by (Pengyan *et al.* 2015). Tensile, charpy and fractography analysis of the samples tested in the H_2S environment revealed a ductile-brittle type of failure. The influence of test environment was explained as the underlying reason for the type of failure mechanism. (Yang *et al.* 2020) investigated the effect of corrosion on tensile fracture property of seamless round steel pipe with an outside of 25 mm and wall thickness of 1 mm. The scaled down dimension was adopted in the work due to the limitation in the load carrying capacity of the test equipment and the cost

implication of using the original pipe material. Tensile test was carried out using a specimen of length 210 mm and a gauge length 50 mm, while the corrosive environment was an accelerated electrochemical corroding set up with 5% NaCl solution as the corroding media. The fracture behaviours of the material is shown in Figure 2.7.

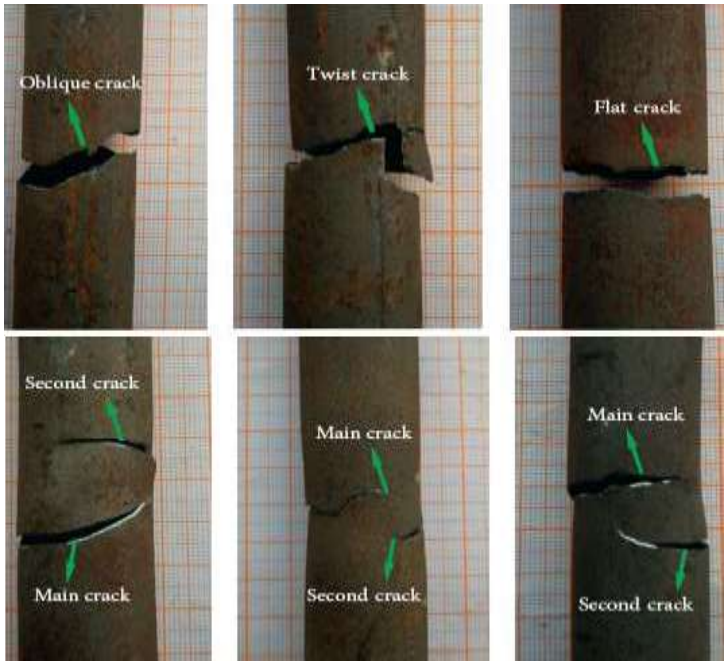

(a) (b)

Figure 2.7: Fracture behaviour of pipe with (a) lower corrosion rates (b) higher corrosion rates (Yang *et al.*, 2020)

From the Figure, it can be seen that the fracture behaviour of pipe with higher corrosion rates have multiple crack initiation sites enhancing the fracture mechanism when compared with specimens that were simulated with lower corrosion rates. For corrosion rates of 10% and 50 %, it was found that the yield and ultimate strengths of the corroded pipe were about 97%, 76% and 97% and 75% of the pipes without corrosion. However, the effect of

temperature on the tensile and fracture behaviour of the pipes was not investigated Yang *et al.* (2020).

Recently, Ike *et al*. (2019) investigated the mechanical and microstructural properties of 20.8 mm thick welded API X70 pipeline steel in air and seawater environments. A double V weld preparation was used and the welding was carried out using manual metal arc welding (MMA) technique in flat (1G) position. A UNITED type universal testing machine was used to carry out the tensile tests while impact testing machine, Vickers hardness tester and scanning electron microscope were used charpy v-notch test, hardness testing and fractography analysis respectively. Microstructure investigation revealed large grains in the steel sample which implies that the material was ductile. When the results samples that were tested in ambient (air) environment were compared with those tested after being exposed to seawater for 12 weeks, it was found that there was 10.5% reduction in tensile strength, 18.7% reduction in compressive strength and about 37% decrease in impact energy. It was also found that hardness values of samples exposed to seawater were significantly reduced when compared with those tested under ambient environment. The implication of the results is that the corrosive seawater environment has a significant effect on mechanical properties of the material.

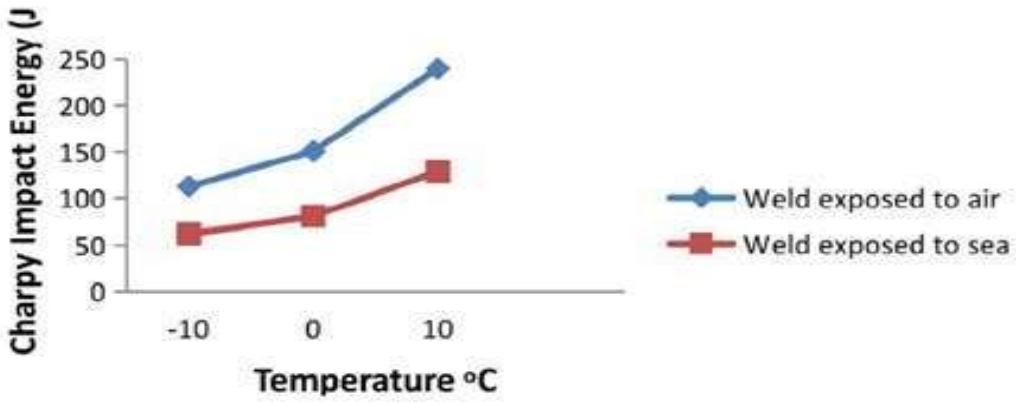

Figure 2.8: Charpy impact energy versus temperature (Ike *et al.*, 2019)

The result of charpy impact energy is compared with the corresponding temperature for weld material exposed to air and seawater as shown in Figure 2.8. The evident effect of environment (seawater) can be seen in the Figure as charpy energy was significantly reduced in seawater across the temperature range considered. However, a wider range of temperature would have been used for testing in order to reveal the effect of temperature on the material charpy impact energy.

Different experimental tests were carried out on API X60, X70 and X100 high strength low alloy (HSLA) steels of dimension 9 mm, 28 mm and 20 mm thickness respectively (Vesga, 2014). Chemical and metallurgical characterization, tensile, charpy V-notch and hardness tests were carried out on the three steels. The chemical characterization of the material was determined by spectroscopic analysis while the metallurgical investigation was carried out using optical microscope, scanning electron microscope (SEM). Hardness tests were carried out using Vickers hardness tester while tensile tests were carried out using 500 kN and 100 kN servohydraulic test machines. The fracture toughness tests were investigated using precracked charpy V-notch specimens at temperatures of –196ºC, –100ºC, –70ºC, –

40ºC, –20ºC and 21ºC. The range of temperatures was achieved by dipping the specimens in liquid nitrogen before testing. Result showed that X70 had higher hardness, yield strength and ultimate strength values that the other steels. The extraction of the X 70 plate from a pipe section and as such the change in the material properties due to work hardening was used as an explanation for the difference in results. With the range of temperature used for testing, the fracture toughness values obtained from the three steels were significantly influenced by temperature with X70 having the highest value followed by X100 and X60 steels respectively. The only set back in (Vesga, 2014) is that no test results were reported for samples that are extracted from weld zones.

2.7 Factors Affecting the Fracture Properties of Pipeline Steels

There are several factors influencing the fracture toughness of engineering materials. It may be experimentally impossible to study the interaction of all these factors considering cost implication and time factor. Apart from temperature and materials modification, some of the factors influencing material fracture toughness are discussed in the next sections. The factors that are discussed in the next sections are not the only factors influencing the fracture properties of pipeline steels. However, they are the ones that are mostly mentioned in the literature.

2.7.1 Stress concentration

The sources of stress concentrations in components and structures are mainly weld imperfections, surface defects, holes and grooves. Cracks initiate at the stress concentration sites and as the crack grows to failure, the stress state is characterized by critical stress intensity factor or fracture toughness. The severity of stress concentrations in welds is characterized by stress concentration factor which is the ratio of the peak or maximum

stress a component/structure experience to the reference or nominal stress (Schijve, 2009). Nominal stresses are the remotely applied stresses while the maximum stress in a component can be determined empirically in the laboratory using strain gauges and numerically by using finite element methods (Schijve, 2009). Stress concentration modifies the stress distribution in a component or structure. The effect of stress concentration induced by corrosion on fracture behaviour of pipelines was studied by (Kim *et al.*, 2019) and a correlation based on stress concentration for estimating the lifetime of pipelines was proposed. The most important factors to be considered when estimating the lifetime of a component with respect to the stress concentration factor are the shapes and types of grooves and imperfections and the type of loading, where the significance of the stress concentration depends on the geometry of the configuration of the notch. A typical nature of how stresses are distributed in a tensile loaded plate with a hole, and a notched plate under bending load is shown in Figure 2.9.

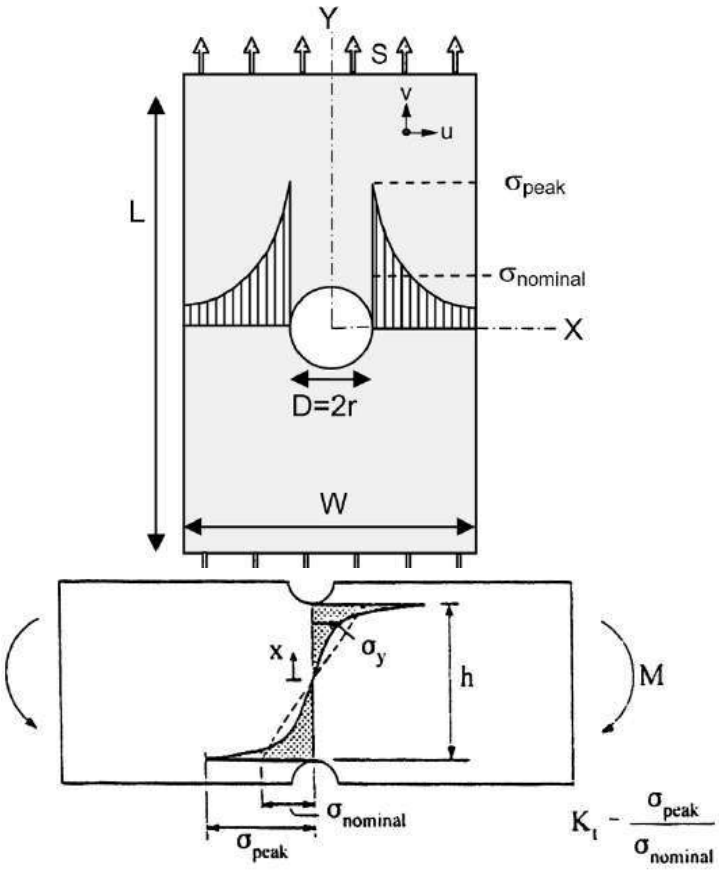

(a) (b)

Figure 2.9: Stress distribution in (a) plate with a center hole under tensile load (b) plate notched at both sides under bending load (Schijve, 2009)

It can be seen from the figure that how stresses are distributed in components or structures do not only depend on the type of loading but on the type of stress raisers. (Murakami, 2019) mentioned that for stress raisers, that the stress at a hole or a notch is expected to be significantly higher that the remotely applied stresses. As such, notched specimens such as those used for fracture toughness tests could experience more stress concentration factors that specimens with a hole due to the severity of stress concentration in the latter. The loads that structures experience when operational could be in tension, compression, torsion or the

combination of the three. Another possible loading scenario that was mentioned (Yang *et al.*, 2020) is the axial loading due to ground motion, landslides or waves which may result in the failure of pipeline by tension or compression. Stress concentration factors for various shapes of groves and type of loading are published in a textbook (Pilkey and Pilkey, 2008).

2.7.2 Material modification by welding, peening and rolling

The term material modification in this context refers to processes such as welding, peening, rolling and their effects on fracture toughness. This thesis is limited to the effect of material modification by welding; however, the mentioned processes will be discussed briefly. Material modification processes are often applied to enhance the integrity of materials. As mentioned earlier, welding has been defined as a process which involves the joining of two similar or dissimilar materials (Palmer and King, 2004). In the process of welding, there are microstructural changes in the material with the expectation that properties such as tensile strength and fracture toughness of the material are enhanced. Therefore, fracture toughness of weldments is expected to be different to the corresponding parent materials due to the former being modified by welding.

In a study carried out by Hashemi (2008), impact tests were conducted on HAZ, parent and seam weld material extracted from X70 steel. The investigation revealed that the toughness energy values were influenced by the material microstructure. The ductile brittle transition temperature for a friction stir welded X80 steel was investigated. Test samples were extracted from three different zone; parent, HAZ and weld materials (Avila *et al*., 2016). The investigation revealed a transition temperature of -100^0C for HAZ and parent materials while for the weld zone, the transition temperature of -60^0C. Analysis of the fracture

surfaces also revealed that the higher fracture energy was associated with ductile fracture surface while the lower fracture energy was associated with ductile-brittle fracture surface. The effect of material modification that was conducted in this study is the investigation of fracture energy in weld charpy V-notch compared to those in parent materials under different temperatures.

Another type of material modification that has been used to enhance the integrity of materials and structures is peening. Peening is a cold working process that is applied to metallic surfaces through a mechanical means in order to improve the material properties. Small, hard or round particles in form of steel shots, ball bearing or glass beads are impacted on the surface (Rudawska, 2019). Peening introduce compressive residual stress through the plastic deformation that is created by the shots on metallic surfaces (Pipinato, 2015) thereby retarding crack formation or growth. It is used in gear teeth, pressure vessels, gas turbines, aircraft parts and structures where the need to improve their fatigue and mechanical strengths are desired.

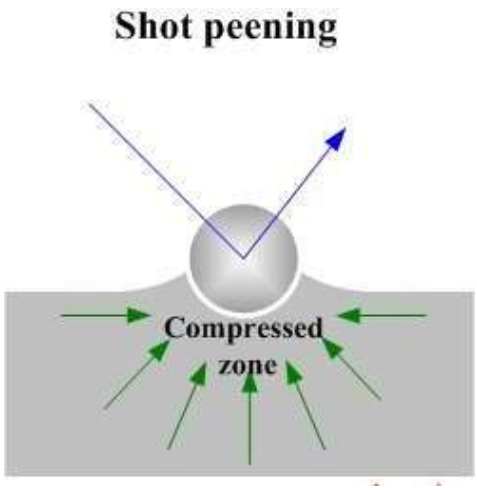

Figure 2.10: Shot peening process (–www.substech.com‖)

There several peening processes such as shot peening, needle peening, ultrasonic peening, laser peening However, the most commonly used among the processes is shot peening where the material to be treated is shot blasted with a velocity range of 40-90 m/s (Rudawska, 2019). An example of shot peening process is shown in Figure 2.10. Another cold working process that is used for material modification is cold rolling where a particular section of the material is cold rolled at a specific load to introduce compressive residual stress and thus enhancing the properties.

2.7.3 Temperature effect

Temperature contributes significantly to fracture properties of pipelines steels and it has been argued in the literature (Vesga, 2014) that fracture properties are reduced as temperature reduces and thus causing a brittle fracture failure mechanism. Most of the works that are reported in the literature investigate charpy impact tests with respect to temperature. The fracture toughness values are determined by correlations that were described previously. However, in some cases, only the charpy energy values are published. For example, the charpy impact energy in 304 stainless steel pipeline used for liquefied natural gas (LNG) transmission was investigated at room temperature to a temperature of -162^0C (Baek *et al.*, 2002). The charpy energy values dropped significantly as the temperature was reduced. (Alfitour *et al.*, 2018) carried out charpy impact, tensile and rockwell hardness tests on API 5L X60 at room 25^0C temperature and at nitrogen cooled temperature (-196^0C). The impact tests were carried out according to the ASTM E 23 standard. There was a significant decrease in the charpy energy values from 210J to 5J when the specimens were cooled in liquid Nitrogen. With the range of temperature used for

testing, Rockwell hardness values increased from 65 to 88, while tensile strengths increased from 498 to 580 MPa.

The effect of temperature on fracture properties of API X65 pipeline steel was also carried out by (Nonn and Brauer 2014) at temperatures of -20 °C -60 °C, -80 °C, -100 °C and -120 °C respectively. Results also showed a significant effect of temperature on charpy V-notch energy values as there was a drop in the values from 216J at -20 °C to 16J at -120 °C for 10 mm thick specimens. However, for 7.5 mm thick specimens, the charpy energy values dropped from 165J at a temperature of -20 °C to 13J at -120 °C. These results also revealed thickness effect on charpy impact energy; and as such suggest that higher impact energy may be absorbed in thicker materials compared to in thinner ones. The results that are discussed in this section also agree with the temperature related fracture behaviour of pipelines steels as investigated in Vesga Rivera work (Vesga, 2014). As mentioned, the set back of most of the investigations that are discussed in this section as well as in previous sections is that fracture properties of weld pipeline steels have not been adequately investigated.

2.7.4 Effect of test environment

The effect of environment is one of the major factors influencing the fracture properties of materials. Pipelines experience highly dynamic harsh environments such as in the soil, seawater; loads and environment from the transporting fluids. The transportation environments include carbon dioxide environment (CO_2) and hydrogen sulphide (H_2S) environment. Therefore, it is expected that the behaviour of pipelines in these environments

will be different since they are site dependent. For example, in seawater environment, there is approximately 3.5% by weight of sodium chloride solution and it was mentioned that natural seawater cannot be entirely replicated appropriately (Shifler and Aylor, 2005). This is due to the variation in contributing factors such as pH, oxygen and temperature. However, CO_2 and H_2S are characterized by the presence of impurities that significantly control the behaviour of materials in these environments.

One of the investigations that compared the effect of test environments on the mechanical and fracture properties of X60, X70 and X100 steels is the work reported in (Vesga, 2014). The steels were exposed to SO_2 and H_2S impurities between 50 to 400 hours. The results showed that regardless of the test temperature used, the energy absorbed by X70 in both environments was more than those absorbed by X100 and X60 steels with X100 steel having higher energy than X60. The influence of environment was also clearly revealed in the values of the charpy energies obtained.

In corrosive environments such as seawater or sodium chloride solutions, mechanical properties of steels are also expected to be different. A study was carried out to investigate the effect of sodium chloride corrosive environment on the properties of round steel pipe (Yang *et al*. 2020). As in a previous section, for 10% and 50 % corrosion rates, results showed that the yield and ultimate strengths of the corroded pipe were 97%, 76% and 97% and 75% of those of the pipes that were not subjected to corrosive environment before testing.

2.7.5 Welding and residual stresses

The failure of welded joints starts from the heat affected zones and progress to the weld and unaffected parent material due weld defects, stress concentrations and weld residual stresses that are introduced due to material thickness, material type and input parameters used during welding. A summary of the location of failure in different grades of pipelines is given in Table 2.3.

Table 2.3 Summary of pipeline failure with their causes and locations (Sharma and Maheshwari 2017)

Material	Cause of failure	Location of failure	Citation
X42	Erosion due to corrosion	Weld metal	(Majid *et al.*, 2010), (Majid *et al.*, 2012), (Majid and Mohsin 2012),
X46	Cracks in fusion zone (slag entrapment)	Weld metal	(Datta and Deva, 2002)
X46	Fatigue crack in weld (residual stress)	Weld metal	(Chapetti *et al.*, 2002)
X46	Defects in weld	Weld metal	(Fazzini *et al.*, 2005)
X46	Hydrogen embrittlement	HAZ	(Azvedo, 2007)
X52	Misalignment of inner and outer weld	Interface of weld & HAZ	Fazzini *et al.*, 2007)
X60	Thinning of wall due to grinding of weld	Weld metal	(Ahmed *et al.*, 2008)
X65	Dents and gouges (Mechanical damage)	Main body of pipe	Macdonald *et al.*, 2007)
X65	Cracks along the toes of the weld due to transit fatigue (residual stress)	Interface of weld & HAZ	(Al-Anezi *et al.*, 2009)
X65	Diffusion of copper at the grain boundary during induction bending operation	Main body of pipe	(Shant *et al.*, 2013)

Investigations that have been carried out on HSLA steels such as X42, X46, X52, X56, X60 and X65 have also revealed that failure in these steels occurred primarily at the weld area and HAZ (Sharma and Maheshwari, 2017). It can be seen from the table that the major sources of these failures have been attributed to weld defects, residual stresses, corrosion and hydrogen embrittlement. Residual stresses are locked up stresses in materials, they can be tensile or compressive in nature and in weld materials, tensile residual stresses are damaging while compressive residual stresses are beneficial to the structure (Adedipe, 2015). The typical behaviour of longitudinal residual stresses in a butt weld is shown in Figure 2.11.

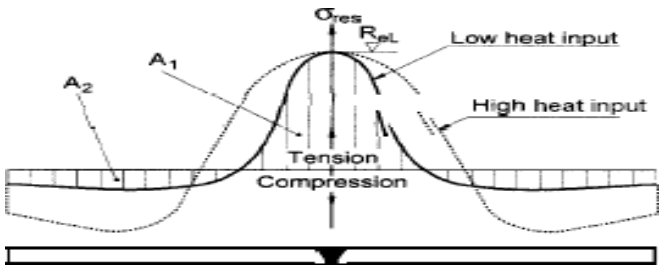

Figure 2.11: Longitudinal residual stresses in a butt weld (Weman, 2003)

It can be seen from the Figure that there are both tensile and compressive residual stress segments in the weld plate. It was mentioned in the literature that the tensile segment of residual stress fields are close to the surface of weld material while the compressive segment usually occur at the middle (Adedipe *et al.*, 2015). It is therefore the responsibility of welding Engineers to first characterize the magnitude of residual stress distribution in a weld structure and to ensure that the aforementioned sources of residual stresses are

optimized during welding in order to improve the life of the structure. Another unforeseen loading scenario occur when residual stresses are present in a welded material under the application of external load is that the locked up residual stresses change the loading pattern on the material as shown in Figure 2.12.

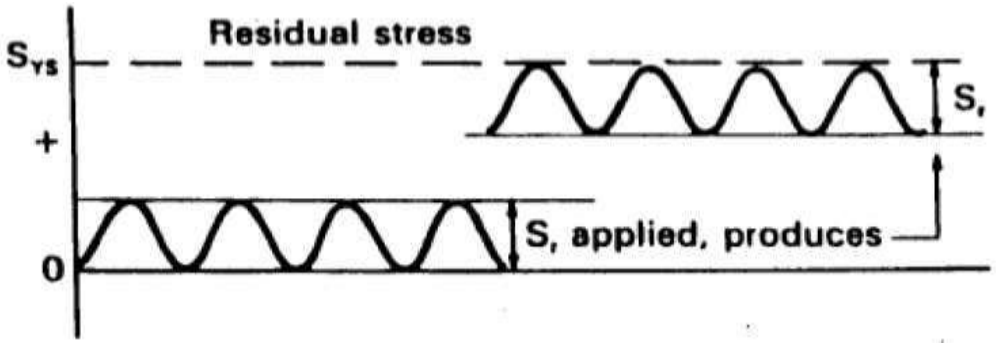

Figure 2.12: Pattern of residual and applied stresses (Kirkhope *et al.,* 1997)

This is probably why some structural welded members fail before meeting their design lives when residual stresses are not taking into account from the design stage. Measurements and characterization or residual stresses are not part of the scope of this research but different ways to measure residual stresses can be found in (Rossini *et al.*, 2012). However, a recognized way to reduce the effect of residual stresses is through post weld heat treatment (PWHT) but due to the level of uncertainties associated with residual stresses, it was mentioned that they cannot be completely removed by PWHT (Kirkhope *et al.,* 1997).

2.7.6 Research gap

In summary, the effect of temperature on fracture toughness of the API X70 steel. Also, the study generated low temperature fracture data using API X70 that can serve as data base for future installation, it also established the lowest temperature of -160°C at fracture energy of 12.3J.

CHAPTER THREE

3.0 MATERIALS AND METHODS

3.1 Materials

The following materials and equipment were used for investigating the fracture properties of the steel used for this research:

1. welded API X70 pipeline steel
2. welding Electrodes
3. liquid Nitrogen

Table 3.1: Equipment

S/N	Equipment	Model	Where available
1	Manual Metal Arc Welding Machine		SSC Workshop Opposite Gwarimpa, Abuja
2	Universal Tensile Testing Machine	United type testing machine	SSC Workshop Ushafa, Abuja
3	Charpy impact testing Machine	Charpy V-Notch Impact Testing Machine	SSC Workshop Ushafa, Abuja
4	Optical Microscope		Oshogbo Machine Tools Osun State
5	Spectroscopic analysis machine		Oshogbo Machine Tools Osun State
6	Scanning electron microscope (SEM)		DICON Kaduna

The materials that were used for investigation was API X70 pipeline steel with a thickness of 20.8 mm, length of 650 mm and width of 310 mm. The material was obtained from the Engineering Materials Testing Facility located at Shabiv Construction Company (SCC) Nigerial Ltd at Ushafa, Bwari, Abuja FCT. The liquid Nitrogen that was used to achieve

the desired temperature during testing was also made available at the testing facility. The material characterisation was carried out at Oshogbo Machine Tools facility in Osun State using the spectroscopic analysis machine.

Tests were carried out on samples that have been modified by welding and the welding was carried out using the manual metal arc welding facility of SCC Abuja. Other equipment that was used for fabrication of test specimens are grinding machine, cutting stone, lathe, electrode designated E7018 and venier caliper. Tensile tests were carried out using the United type universal tensile testing machine belonging to the Pipe Testing Facility of SCC Abuja. The tensile test machine used is shown in Plate I. Impact tests were carried out using the Charpy V-notch Impact Tester located at SCC Abuja (Plate II), while the notch of the specimens was prepared using Blacks Charpy V-notch prepration machine. This is shown in Plate III



Plate I: United type universal testing machine



Plate II: Charpy V-notch impact testing machine



Plate III: Blacks Chapy V-notch machine

3.2 Methods

The methods applied is categorized into two which includes chemical analysis of the material by spectroscopic method and welding and specimen method.

3.2.1 Chemical analysis of API X70 steel by spectroscopic method

The chemical composition of API X70 was carried out using the method reported by Ike *et al.,* (2019). However, in order to ensure the conformity of the material composition with the previous studies and also to the API requirements, a confirmatory test was carried out through microstructure examination to obtain the chemical composition of the material. The chemical analysis result is presented in chapter 4.

3.2.2 Welding and specimens preparation

The welding of the 20.8 mm thick weld plate was carried out using manual metal arc welding in flat welding position (1G) at the Welding Facility of SCC Abuja. The weld steel plate was cleaned using a soft wire brush to avoid any impurities that may be trapped in the joint during welding. The edge preparation was designed based on the recommendation given by the SCC for welding pipe steels. The groove angle was 60^0 and a root face of 6 mm and root spacing of 0.3 mm were used. The weld plate edge preparation is shown in Figure 3.1. After the edge preparation had been achieved, manual metal arc welding technique was used to fill up the weld using an electrode designated E7018 and with a wire diameter of 4 mm.

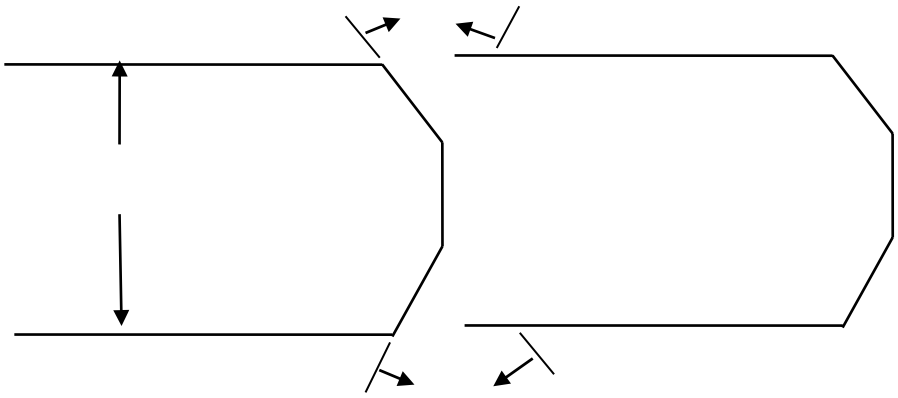

Figure 3.1: Weld plate edge preparation

3.3 Charpy Specimens Extraction and Testing

After the welding had been completed, the specimens that are used for testing were extracted from the welded plate. The extracted Charpy V-notch samples were designed according to ASTM E23 (ASTM E 23 2014), with a notch radius of 0.25 mm. The notches of the samples were prepared using the Blacks charpy V-notch machine shown in plate 3.3. Parent or base specimens were extracted with their notches on the parent material as shown in Figure 3.2.

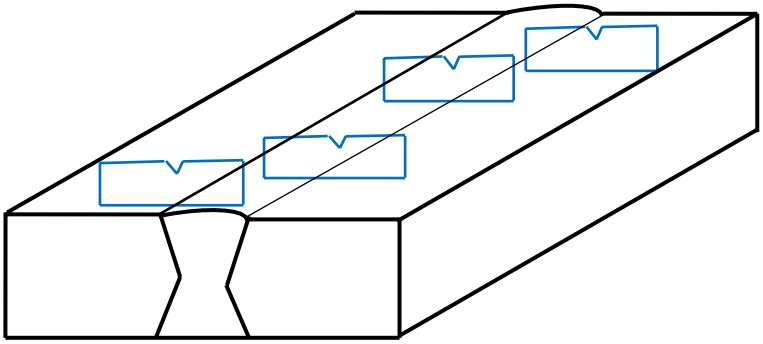

Figure 3.2: Chapy V-notch specimens

Similarly, in order to investigate the effect of material modification by welding on the fracture behaviour of the API X70 steel, charpy samples were extracted with their notched positioned on the weld area of the plate as shown in Figure 3.2. The dimensions of the designed charpy V-notch specimens are given in Figure 3.3. The sample was 55 mm in length and with a thickness of 10 mm, while the depth of the V-notch was 2 mm with a radius of 0.25 mm. Plate IV shows the specimens that were extracted from the parent plate as well as from the weld area.

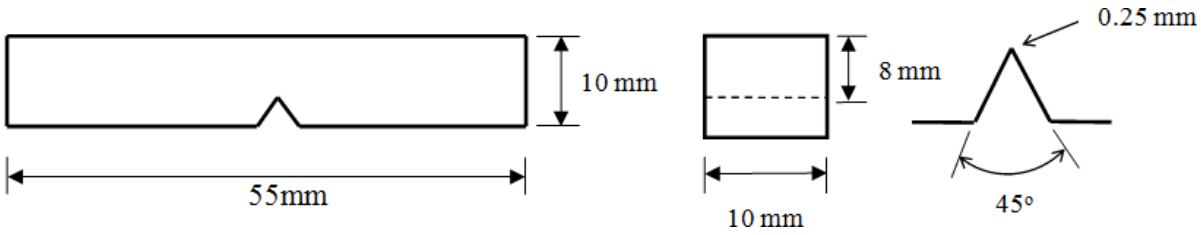

Figure 3.3: Charpy V-notch geometry



Plate IV: Extracted charpy V-notch specimens from parent plate and weld area

The impact tests were carried out according to the specifications set out in the ASTM E23 (ASTM E 23 2014) using the impact testing machine shown in plate 3.2. Tests were carried out at temperatures of -10°C, -20 ^{o}C, -40 ^{o}C, -60 ^{o}C, -80 ^{o}C, -100 ^{o}C, -120 ^{o}C, -160 ^{o}C, 0 ^{o}C, 10 ^{o}C and 20 ^{o}C (Vegas, 2014). The lowest temperature that could be achieved by the liquid nitrogen was -160 ^{o}C and this informed the choice of temperatures used for testing. After achieving an initial temperature of -160 ^{o}C, the specimen was removed from the liquid nitrogen jar and was mounted on the testing area of the impact testing machine. The pendulum was released to strike the specimen after a desired temperature had been achieved. The temperature was monitored using a hand-held infrared thermometer. After the impact load was applied through the pendulum to break the specimen, the energy that was absorbed by the specimen was recorded from the gauge of the machine. The process was repeated for both parent and weld specimens. The energies absorbed by the specimens were plotted against the test temperatures. Scanning electron microscope (SEM) analyses were carried out on the surfaces using the SEM available at Defence Industries Corporation of Nigeria (DICON) Kaduna.

3.3.1 Tensile specimens extraction and testing

It will be recalled from chapter 2 section 2.2 that two of the correlations that were used in the literature to estimate the fracture toughness of materials require information of the yield strengths. These correlations were developed by Barsom and Rolfe (1999) and Roberts and Newton (1984). Due to the required yield strength values, specimens were extracted from both parent and weld areas in order to obtain the yield strengths.



Plate V: Parent tensile test specimens



Plate VI: Weld tensile test specimens

The extracted parent tensile tests specimens are shown in Plate V, while the extracted weld tensile test specimens are shown in Plate VI. It was ensured that the gauge section of the weld specimens encompassed the weld area of the plate. The specimens were designed according to the specifications in the ASTM E8 (ASTM E8 2013); and a design of the weld specimen is shown in Figure 3.4 with the weld line located at the guage section (Figure 3.4). The parent test specimens do not have the weld groove at the gauge section. Tensile

tests were carried out at room temperature using the United type universal testing machine shown in Plate I

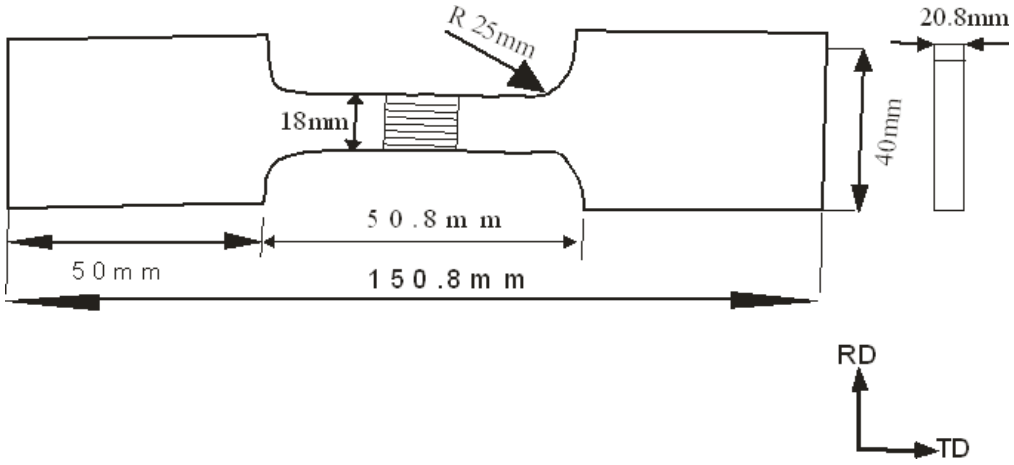

Figure 3.4: Weld tensile test specimen design

The yield strengths were determined from the relationship of stress and strain values as recommended by the ASTM E8 (ASTM E8 2013). The determination of yield strength was carried out at room temperature, therefore the value of the yield strengths used for the estimation of fracture toughness values are those that were carried out in the normal laboratory condition.

3.3.2 Fracture toughness calculation using charpy V-notch correlations

Fracture toughness of the material was determined using the charpy V-notch correlations that were presented in chapter 2 section 2.2. The equations are outlined next. The one described in BS 7910 (BS 7910 2013) is given in Equation 3.1.

$$K_{mat} = [(12\sqrt{\overline{C_v}} - 20)\left(\frac{25}{B}\right)^{0.25}] + 20 \qquad (3.1)$$

Where:

K_{mat} is the estimated fracture toughness ($MPa\sqrt{m}$)

B is thickness of the material (mm)

C_v is lower bound Charpy V-notch impact energy at the service temperature (J)

Fracture toughness of the material used for this research was also calculated for lower shelf or lower transition temperature correlations using Equation 3.2 to 3.6.

$$K_{IC}^2 = 45.1 * CVN^{1.5} \quad \text{(Barsom and Rolfe, 1970)} \qquad (3.2)$$

$$K_{IC}^2 = 105 * CVN \quad \text{(Barsom and Rolfe, 1970)} \qquad (3.3)$$

K_{IC} is fracture toughness of the material ($MPa\sqrt{m}$)

CVN is Charpy v-notch energy (J).

$$K_{IC} = 14.6 * (CVN)^{0.5} \quad \text{(Sailors and Corten 1972)} \qquad (3.4)$$

$$K_{IC} = 19 * (CVN)^{0.5} \quad \text{(Marandet and Sanz 1977)} \qquad (3.5)$$

$$K_{IC} = 8.47 * (CVN)^{0.63} \quad \text{(Roberts and Newton 1984)} \qquad (3.6)$$

Upper shelf fracture toughness was also calculated in relation with material yield strength using Equation 3.7 and 3.8.

$$\left(\frac{K_{IC}}{\sigma_{ys}}\right)^2 = 0.64 * \left(\frac{CVN}{\sigma_{ys}} - 0.01\right) \quad \text{(Barsom and Rolfe 1999)} \qquad (3.7)$$

$$K_{IC} = 0.804\sigma_{ys} * \left(\frac{CVN}{\sigma_{ys}} - 0.098\right)^{0.5} \quad \text{(Roberts and Newton 1984)} \qquad (3.8)$$

Where σ_{ys} = yield stress of the material (MPa).

CHAPTER FOUR

4.0 RESULTS AND DISCUSSION

4.1 Spectroscopic Analysis of Results

Spectroscopic revealed the chemical composition of the steel material as set out in Table 4.1. The essence of this analysis was to establish the material conformity with the chemical analysis that was presented in a previous study as shown in Table 4.2 (Ike *et al*. 2019).

Table 4.1: Chemical composition of API X70 steel

Element	C	Si	Mn	P	S	Cr	Ni	Cu	Al	V	Mo	Ti	Nb	N	Ca	B
Weight(%)	0.045	0.17	1.53	0.003	<0.003	0.248	<0.005	<0.002	0.018	0.014	0.110	0.020	0.051	0.004	0.0022	0.0026

Table 4.2: Chemical composition of API X70 steel (Ike *et al*., 2019)

Element	C	Si	Mn	S	Cr	Ni	Cu	Al	V	Mo
Weight (%)	0.051	0.210	1.510	0.002	0.240	0.010	0.002	0.048	0.021	0.118

It can be seen from Table 4.1 that the chemical analysis that was carried out in the present investigation compare well with the results presented in (Ike *et al*. 2019). The variation of some of the elements may be as a result of experimental condition. The result was also

compared with those reported in literature for the same material (Godefroid *et al*. 2014; Vesga, 2014). The value obtained for manganese weight in this study was though lower than what was (1.89%) reported by (Vesgas, 2014). It compared well with the result (1.536%) of Godefroid *et al*. (2014). The carbon content was also found to be within the same range. The marginal 0.051 difference in the result could be as a result of the type of procedure used in manufacturing the steel materials. The results presented by (Omale, 2016) for a similar steel material also show good agreement with the present results. Comparing the chemical analysis results of the steel used in this research with those published in the literature, it appears that the steel satisfies the API requirements.

4.2 Charpy V-Notch Test Results and Discussion

Figure 4.1 shows the plot charpy V-notch test results against the corresponding test temperature. The charpy energy dropped from 145.6 J to 12.3 J as the test temperatures were reduced from 20 ^{o}C to -160 ^{o}C which implies that energy absorbed during charpy test is sensitive to temperature. The charpy energy values obtained from the present material and their reduction with respect to lower temperature agree with the fracture behaviour of studies that are reported in chapter 2. These includes the investigations carried out by Ike *et al.* (2019), Baek *et al*. (2002), Alfitour *et al.* (2018), Vesga, (2014) and Nonn and Brauer, (2014). For example, in Baek *et al.* (2002), charpy energy was found to reduce from 210 J at a temperature of 25°C to 5 J at a temperature of -196 ^{o}C while in Nonn and Brauer (2014), charpy impact energy reduced form 216 Jat a temperature of 20°C to 16 J at a temperature of -120 ^{o}C.

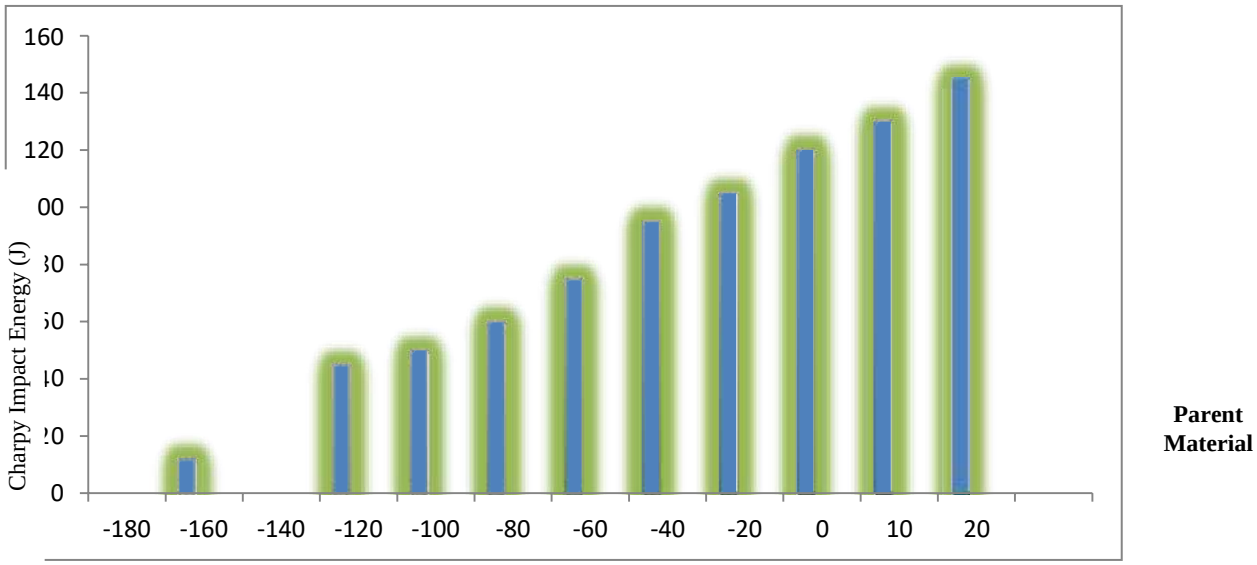

Figure 4.1: Charpy V-notch energy a Temperature ^{0}C materials with Temperature

In the present study charpy impact enenegy in parent material reduced from 145.6 J at a temperature of 20°C to 12.3 J at a temperature of -120 ^{o}C. This implies that temperature has a significant effect on fracture behaviour of materials which can be seen by the reduction in charpy energies significantly. It can also be seen that the reduction in charpy energy is more pronounced at lower temperatures than in higher ones. It was also observed that the charpy energy obtained in the present study are higher than those obtained in (Vesga, 2014). This may be attributed to the sensitivity of the specimen notch. In (Vesga, 2014), precracked specimens were used for testing and precracking minimizes the effect of the notch and hence the correponding data (ASTM E647 2008). In this study, the specimens were not precracked; therefore the notch sensitivity would have influenced the absorbed energy. If the specimens were not notched at all, then it is expected that absorbed

energy would be considerable higher. Sensitivity of specimen notch to absorbed energy was also observed for API X60 steel as higher energy was obtained in unnotched specimens than in notched ones (Alfitour *et al*., 2018).

Figure 4.2 presents the charpy energy absorbed from weld materials with respect to test temperature. Similarly, the enegry values reduced with reduction in temperature across the range of temperature used for testing. It was found that the change in charpy energy with respect to temperature in weld has a similar trend with those obtained in parent material (Figure 4.1).

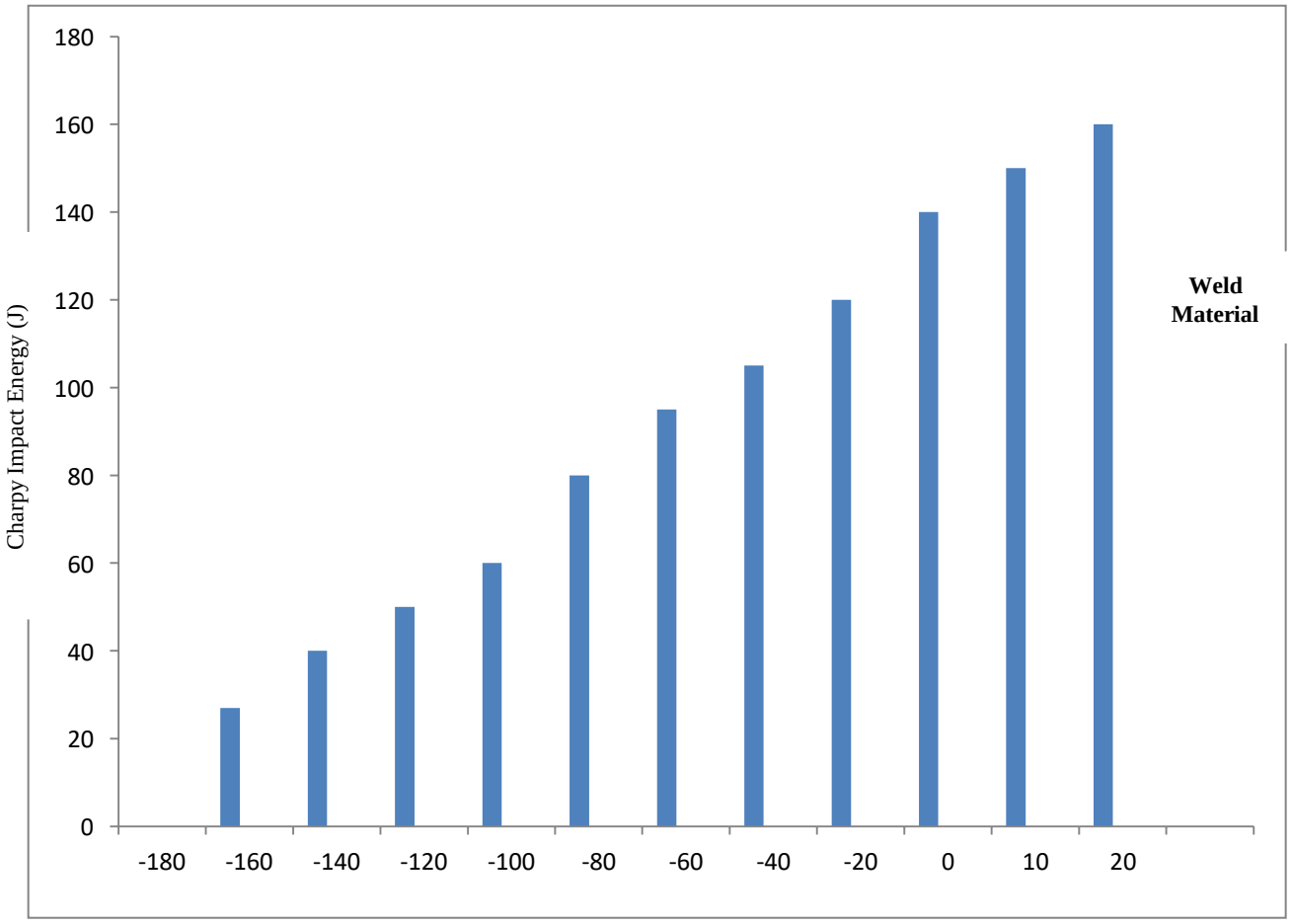

Figure 4.2: Charpy V-notch energy absorbed in weld materials with Temperature

Based on the explanation given in BS7910, the lower shelf/transition behaviour regarding the master curve was determined with respect to temperatures for charpy energies of 27 J and 40J respectively. From this study, these temperatures can be found to be between -100°C to -160°C for parent and weld materials. As such lower temperature that are not within the range used in this study would be part lower transition temperature. However, the master curve was not used due to limited data as same was designed to address a lot of scatter on the conventional charpy energy versus temperature (BS 7910 2013). This may be considered a limitation of the present study.

Figure 4.3 compares the charpy energy obtained in parent material with those obtained in weld. It can be seen that the energy absorbed in weld materials are higher than those obtained in parent material across the test temperatures. The mean of the difference in charpy energy absorbed across the test temperatures was found to be 28.02J. At temperatures of 20°C and 10°C, the percentage difference of the absorbed energy in parent compared to in weld was found to be 20% which was approximately a quarter of the enegry absorbed in weld material at the mentiones temperatures. At temperatures of -10°C and -20°C, the percentage difference in the absorbed energy was found to be 18% while at temperatures of -40°C, -60°C and -80°C the percentage difference in the absorbed energy was approximately 23%. The highest percentage difference in absorbed energy between the parent and weld material was obtained at the temperature of -160°C which was found to be 36%.

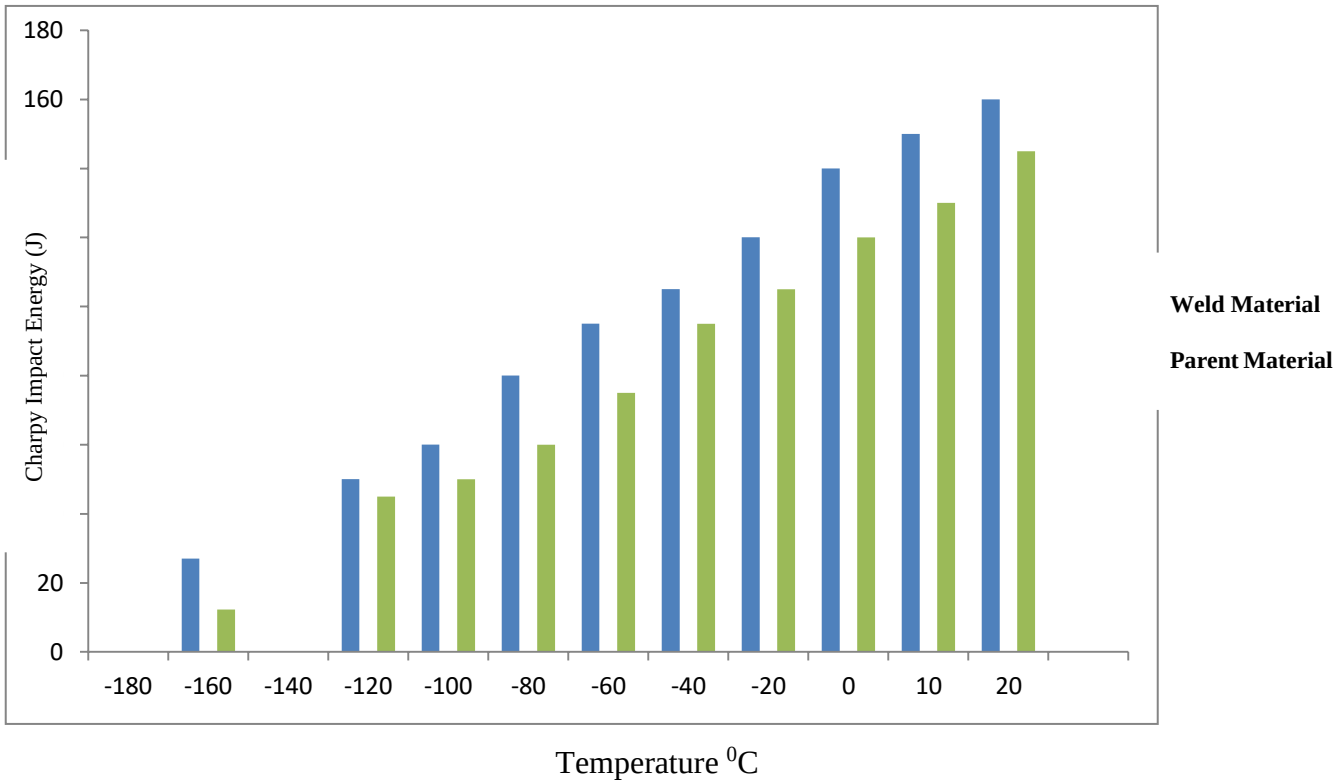

Figure 4.3: Comparison of Charpy energy absorbed in parent and weld materials with Temperature

As such, there was no specific trend in the percentage differences between the energy absorbed in the parent and weld materials. However, the differences in the higher temperature observed in the weld compared to in parent materials may be due to the influence of material modification by welding. Figure 4.4 shows the typical fractured specimens extracted from parent and weld materials.



(a) (b)

Plate VII: Fractured surfaces of (a) parent's specimens, (b) weld specimens

Welding irrespective of the type used alters or modifies material microstructure and in essence refines the grains due to different weld layers which are placed on each other during welding. Therefore, properties such as fracture toughness, tensile and yield stresses may be enhanced by welding due to grain refinement by microstructural changes and hence causing an increase in toughness of the weld material. It can be observed from Figure 4.4(a) that the surfaces of the fractured parent specimens are flat and the specimens were broken completely which shows the characteristic brittle fracture behaviour under cold temperature, while the weld specimen surfaces (Figure 4.4 b) show a little ductile-brittle fracture with uncracked ligament compared to the entirely flat surfaces that was revealed in parent materials. This implies that the due to microstructure changes and material variation induced by welding, weld materials were tougher than the corresponding parent materials;

and this may be one of the reasons why higher energies were absorbed in weld than in parent materials. It was also mentioned in Hashemi (2008) that material microstructure influenced the fracture energy values obtained from HAZ, parent and seam weld material extracted from X70 steel. Even in plain materials, (Cheng and Xue, 2011) mentioned that microstructure influenced the fracture properties of X70 and X80 steels significantly. Contribution of the filler material used for welding is another factor that could influence material properties as it is possible to alter the number of individual elements in the material composition of the material during welding. A similar explanation was given with respect to grain refinements in X70 steel (Godefroid *et al*. 2014). Sharma and Maheshwari (2017) also stated that the microstructure of welds is determined by the chemical composition of the parent material, heat applied during welding and the chemical composition of the filler materials. Therefore, the weld data gotten from this study could have been influenced by these aforementioned factors.

Figure 4.5 shows the scanning electron microscope (SEM) analysis that was carried out on the fractured surfaces of parent and weld specimens.

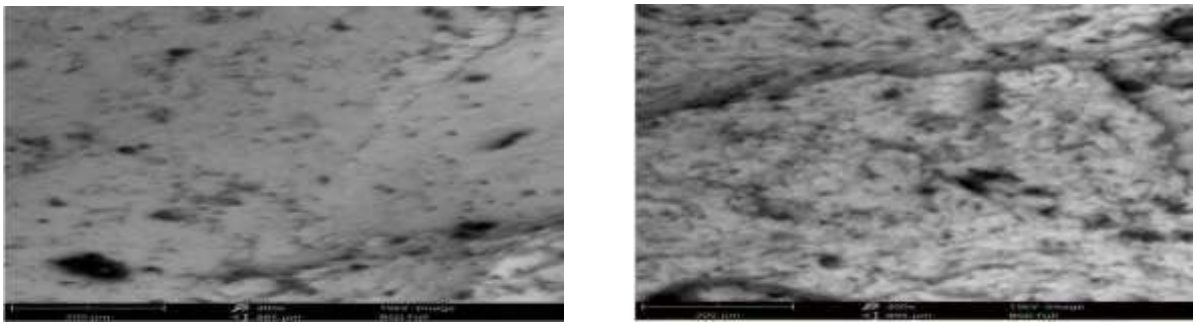

(a) (b)

Figure 4.4: SEM analysis of (a) parent's specimens, (b) weld specimens

Generally, analysis of the specimens broken at both higher temperatures and lower temperature of -120°C to -160°C revealed flat uniform surfaces for parent material (Figure 4.5a) and surfaces characterized by some dimples and irregular nature as shown in Figure 4.5 b. The black spots on the surfaces may be due to the later effect of liquid nitrogen on the surfaces after soaking. The SEM machine used was limited to 200 μm, as such, more SEM analyses are required in future research in order to characterize the surfaces further with respect to clearer resolution and fracture surfaces appearance.

Another factor that may influence the results that are compared in Figure 4.3 is the effect of residual stresses. As mentioned in chapter 2, residual stresses has been attributed to the cause of most failures in pipelines Sharma and Maheshwari (2017). For the energy absorbed in the weld material of the present study, it is possible that the fracture region of the specimens coincided with the better residual stress profile region and hence resulted in higher energy absorbed in weld compared to in parent material.

4.3 Tensile Test Results and Discussion

The essence of the determined of tensile properties of the steel used for investigation is to establish the yield strength that would be used to calculate fracture toughness using Equations 3.7 and 3.8. As mentioned in chapter 3, the tensile property of the material was determined at room temperature. There was no facility attached to the tensile test machine to control the specimen temperature while the tensile test was being carried out.

Tables 4.3 and 4.4 show the tensile properties of parent and weld materials. Five specimens were tested for each material microstructure as described in chapter 3. The mean yield and strength as well as the mean yield/tensile ratio of the parent materials were determined to

be 561.05 MPa, 632.50 MPa and 0.89 respectively. These results when compared with the results obtained using similar materials in the literature Shin *et al.* (2009), Godefroid *et al.* (2014) and Ike *et al*. (2019) revealed good agreement. The mean tensile and yield strengths obtained by Shin et al. 2009 for samples taken from different microstructure of API X70 were 516 MPa and 644 MPa respectively, while in Godefroid *et al.* (2014), the yield and tensile strength were 586MPa and 640 MPa. However, in Ike *et al.* (2019), the mean yield and tensile strenghts were 573.05 MPa and 651.57 MPa respectively. It can be seen that these results are close to those obtained form the present study.

Specimen Number	Yield strength (MPa)	Tensile strength (MPa)	Yield/Tensile Ratio
1	558.46	645.30	0.87
2	564.35	638.15	0.88
3	568.84	634.33	0.90
4	545.33	623.45	0.87
5	568.25	621.27	0.91

Table 4.3 Tensile properties of base material

Similarly, the mean yield and strength; and the mean yield/tensile ratio of the weld materials for the results shown in Table 4.4 were determined to be 575.69 MPa, 668.61 MPa and 0.86 respectively. In Ike *et al.* 2019, the mean yield and tensile strengths for weld materials were 591.95 MPa and 680.62 MPa respectively. It can be seen that these results and those obtained from the present study are close; with the variation which may be due to changes in experimental conditions. It can also be seen that for all the specimens tested, the yield and tensile strengths of weld material (Table 4.4) are higher than those obtained from parent materials (Table 4.3).

Table 4.4 Tensile properties of weld material

Specimen Number	Yield strength (MPa)	Tensile strength (MPa)	Yield/Tensile Ratio
1	576.55	685.25	0.84
2	581.25	693.25	0.84
3	575.85	665.54	0.87
4	564.65	655.85	0.86
5	580.15	643.15	0.90

The difference between the mean yield and tensile strengths for parent and weld materials were determined to be 14.64 MPa and 36.11 Mpa respectively. As mentioned in section 4.2, grain refinement of the weld material due to welding, the associated welding parameters and the contribution to the toughness due to chemical composition of the filler material could be possible for the higher strengths in weld materials that in parent materials. Also, the effect of residual stresses introduced during the welding would have also contributed to the tensile properties of the weld materials due to the different cooling rates associated with welding.

4.4 Fracture Toughness Results and Discussion

Figure 4.6 shows the plot of calculated fracture toughness against charpy energy values. The values plotted in the Figure were obtained using Equations 3.1 to 3.6. For parent materials, the fracture toughness using the BS 7910 correlation was found to be in the range 176.92 $MPa\sqrt{m}$ at 20°C to 47.77 $MPa\sqrt{m}$ at -160°C. Only Sailors and Corten correlation (Sailors and Corten 1972) agree well with the BS 7910 correlation with fracture toughness in the range of 176.17 $MPa\sqrt{m}$ at 20°C to 51.20 $MPa\sqrt{m}$ at -160°C. This can be seen in Figure 4.6 as the data points of the two correlations fall on one another. Using the BS 7910 as a baseline for conservative prediction of fracture toughness as mentioned in (BS 7910

2013), it can be seen from Figure 4.6 that Barsom and Rolfe (1970) Equation 3.2; and Marandet and Sanz 1997 Equation 3.5 correlations overestimated the fracture toughness and as hence may give unconservative predictions for the case considered in this study.

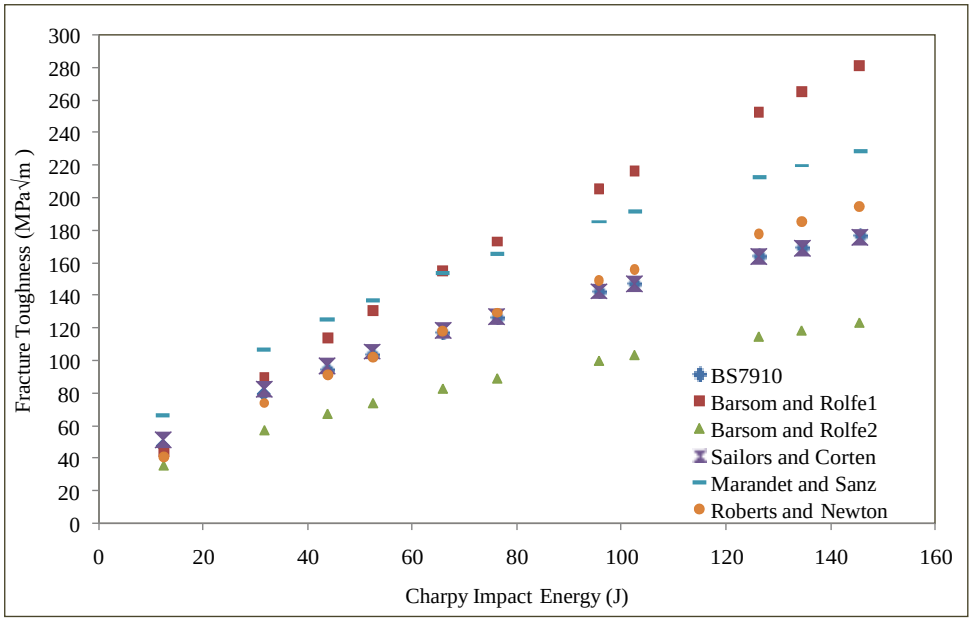

Figure 4.5: Fracture toughness-Charpy energy correlation for parent material

It can also be seen from the Figure that Robert and Newton correlation (Roberts and Newton 1984) (Equation 3.6) agree with BS 7910 correlation (Equation 3.1) but not as close as the values obtained using Sailors and Corten correlation, as the calculated fracture toughness was in the range 195.29 $MPa\sqrt{m}$ at 20°C to 41.16 $MPa\sqrt{m}$ at -160°C. Barsom and Rolfe correlation (Barsom and Rolfe 1970) (Equation 3.3) under estimated the predictions of BS 7910 as the fracture toughness values were in the range 123.64 $MPa\sqrt{m}$ at 20°C to 35.94 $MPa\sqrt{m}$ at -160°C. However, for design purpose and for a conservative prediction, Barsom and Rolfe correlation could still be applied if the BS 7910 correlation is used as a baseline. For parent materials, the mean error between fracture toughness

determined by BS 7910 correlation (Equation 3.1) and those determined by Equations 3.2 to 3.6 were found to be 35.9%, 28.9%, 1.5%, 31.9%, 6.2% respectively. Judging from the mean errors, in this study, it has also shown that Sailors and Corten correlation (Equation 3.4) and Robert and Newton correlation (Equation 3.6) are reliable correlations and thus agree with the BS 7910 guidance regarding the estimation of fracture toughness from charpy V-notch energy.

Figure 4.7 shows the plot of calculated fracture toughness versus the obtained charpy V-notch energy from weld materials. It can be observed from the figure that at lower charpy energy values, the variation in the correlations is small compared to the significant variation which occurs as the charpy energy increased to higher values. The smaller variation at lower energy could be explained by the influence of temperature on energy absorbed. This implies that for arctic region or deeper water depths which are characterized with lower temperatures, the resistance of the present material to fracture would be considerable low. Therefore, for inspection relating to fracture analysis, a regular assessment of pipeline operating in colder regions may be necessary compared to those installed in less harsh environment.

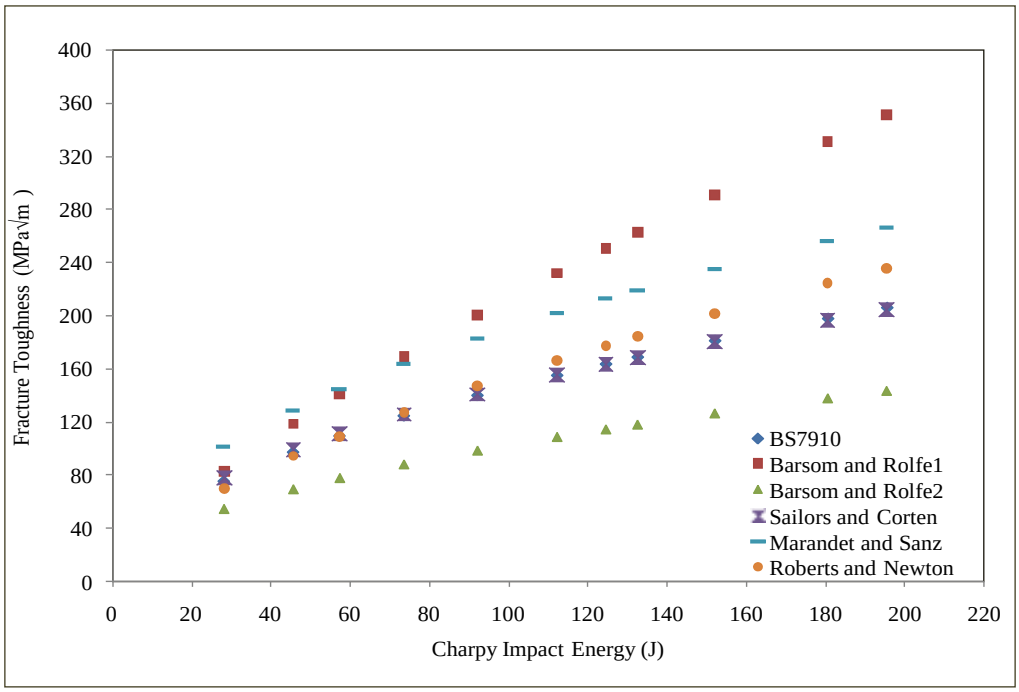

Figure 4.6: Fracture toughness-Charpy energy correlation for weld material

The obtained fracture toughness of weld materials using BS 7910 correlation was found to be in the range of 205.83 $MPa\sqrt{m}$ at 20°C to 74.98 $MPa\sqrt{m}$ at -160°C. As shown for parent materials, Sailors and Corten (Sailors and Corten 1972) correlation (Equation 3.4) agree with the BS 7910 recommendation as the calculated fracture toughness was in the range of 204.14 $MPa\sqrt{m}$ at 20°C to 77.53 $MPa\sqrt{m}$ at -160°C. Similarly, as shown in Figure 4.7, Robert and Newton correlation (Roberts and Newton 1984) agree with BS 7910 correlation (Equation 3.1) but not as close as the values obtained using Sailors and Corten correlation. The calculated fracture toughness was in the range 235.13 $MPa\sqrt{m}$ at 20°C to 69.43 $MPa\sqrt{m}$ at -160°C. As mentioned earlier, if BS 7910 recommendation (BS 7910 2013) is considered as a baseline for conservative prediction of fracture toughness, the data plotted in Figure 4.7 shows that Barsom and Rolfe (Equation 3.2); and Marandet and Sanz

(Equation 3.5) correlations overestimated the fracture toughness of weld materials. Hence, these equations may give unconservative prediction during fracture assessment for the cases (Parent and weld materials) considered in this study. It can also be observed from the figure that Barsom and Rolfe correlation (Barsom and Rolfe 1970) under estimated the BS 7910 recommended equation as the fracture toughness values were in the range 143.27 $MPa\sqrt{m}$ at 20°C to 54.42 $MPa\sqrt{m}$ at -160°C. Therefore, Equation 3.3 could still be applied for fracture assessment of the present material within the range of temperature used if the BS 7910 recommendation is considered as baseline. The error analysis that was carried out revealed that for weld materials, the mean error between fracture toughness by BS 7910 correlation (Equation 3.1) and those determined by Equations 3.2 to 3.6 were 45.1%, 29.5%, 0.9%, 30.7% and 7.4% respectively.

The results of variation of the fracture toughness with the range of temperatures, for parent and weld materials are shown in Table AI in Appendix I. The fracture toughness test results using the Equations 3.7 and 3.8 (Barsom and Rolfe 1999) (Roberts and Newton 1984), which are related to the yield stress of the material returned error values particularly for (Roberts and Newton 1984) correlations. This was evident at lower temperature range of -80°C to -160°C for parent materials and -100°C to -160°C for weld materials respectively. The results did not compare well with the results of other correlations that were discussed earlier. Hence, these results were not plotted in Figures 4.6 and 4.7 but they are shown in Table A II, Appendix I.

CHAPTER FIVE

5.0 CONCLUSIONS AND RECOMMENDATIONS

5.1 Conclusions

Base on the experiments carried out in this research including microstructural examination by SEM, Spectroscopic analysis, and impact tests, the following conclusions may be drawn.

1. Large grain sizes were observed in the microstructure of the sample API X70 steel plate and that implies that the steel was ductile since large grains give room for large amounts of slip to occur thus giving better ductility.
2. The API X70 steel base metal composed of carbon (0.045wt% C), silicon (0.17wt% Si), manganese (1.53wt% Mn), phosphorus (0.003wt% P), sulphur (<0.003wt% S), chromium (0.248wt% Cr), Nickel (<0.005wt% Ni), copper (<0.002wt% Cu), aluminum (0.018wt% Al), vanadium (0.014wt% V), molybdenum (0.110wt% Mo), titanium (0.022wt% Ti), (0.051wt%Nb), nitrogen (0.004wt% N), calcium (0.0022wt%), Boron (0.0026wt% B). The API X70 is therefore classified as low carbon steel with alloying elements (Mn, V, Cr, Si, Ni, Mo and Cu) that help in the strengthening of the ferrite.
3. Charpy energy results were determined for both the parent and weld specimens. Impact tests were determined at temperatures -10^0C, -20^0C, -40^0C, -60^0C, -80^0C, -100^0C, -120^0C, -160^0C, 0^0C, 10^0C, and 20^0C. The charpy energy dropped from 145.6 J to 12.3 J as the test temperature were reduced from 20^0C to -160^0C which implies that energy absorbed during charpy test is sensitive to temperature.

4. The tensile properties of parent and weld materials were determined at room temperature. Five specimens were tested for each material microstructure. The mean yield and strength as well as the mean yield/tensile ratio of the parent materials were determined to be 561.05Mpa, 632.50Mpa and 0.89 respectively. Meanwhile, the mean yield and strength, and the mean yield/tensile ratio of the weld materials were determined to be 575.69Mpa, 668.61Mpa and 0.86 respectively.
5. The fracture toughness of the API X70 steel using charpy V-notch correlations were determined for both parent and weld materials. For parent materials, the fracture toughness using the BS 7910 correlation was found to be in the range 176.92Mpa√m at 20^0C to 47.77Mpa√m at -160^0C. The fracture toughness of weld materials using BS 7910 correlation was found to be in the range of 205.83Mpa√m at 20^0C to 74.98Mpa√m at -160^0C.

5.2 Recommendations

(i) The study should be conducted on the higher strength alloy steels such as X80, X100 and X120

(ii) The study of effect of temperature on fracture behavior of API X70 steel as modified by welding on tropical region should be carried out to determine and compare the rate of fracture toughness of parent and weld materials. It will help to predict life of the metal at the region.

5.3 Contribution to knowledge

i. The study established the effect of temperature on fracture toughness of the API X70 steel

ii. The study generated low temperature fracture data using that can serve as database for future installation. It also establishes the lowest temperature of -160^0C at fracture energy of 12.3 J.

REFERENCES

Adedipe, O., Brennan, F. & Kolios, A. (2015). Corrosion Fatigue Crack Growth in Offshore Wind Monopile steel HAZ Material. In *Analysis and Design of Marine Structures V, 5th International Conference on Marine Structures,* 207–12. Southampton, United Kingdom: Taylor and Francis Group.

Adedipe, O. (2015). *Integrity of Offshore Structures.* (Unpublished PhD Thesis). Cranfield University, United Kingdom

Adegbite, M. A. (2014). *Flow Accelerated Preferential Weld Corrosion OF X65 STEEL in Brine Containing Carbon Dioxide and Oxygen*. (Published PhD Thesis). Cranfield University, United Kingdom.

Alfitouri, A. O., Savas, M. A. & Evcil, A. (2018). Charpy Impact and Tension Tests of Two Pipeline Materials at Room and Cryogenic Temperatures. *International Journal of Applied Engineering Research* 13 (17): 13321–34.

Aliu, S. (2012). Investigation of Mechanical and Microstructural Properties of Welded Joint of Nigerian National Petroleum Corporation Pipelines. (Unpublished masters Thesis). Federal University of Technology Minna, Nigeria.

Anderson, T. L. (2005). *Fracture Mechanics Fundamentals and Applications*. Third Edit. Taylor and Francis Group.

API Energy. (2008). Comparison of API Spec 5L 43rd Edition and ISO 3183, Second Ed.

ASTM E 23. (2014). Standard Test Methods for Notched Bar Impact Testing of Metallic Materials.

ASTM E647. (2008). Standard Test Method for Measurement of Fatigue Crack Growth Rates.

ASTM E8. (2013). Standard Test Methods for Tension Testing of Metallic Materials.

Avila, J. A., Lucon, E., Sowards, J., Mei, P. R & Ramirez, A. J. (2016). Assessment of Ductile-to-Brittle Transition Behavior of Localized Microstructural Regions in a Friction-Stir Welded X80 Pipeline Steel with Miniaturized Charpy V-Notch. *Journal of Testing, Metallurgical and Materials Transactions* 47: 2855–2865.

Baek, J., Kim, Y., Kim, W. & Kho, Y. T. (2002). Effect of temperature on the charpy impact and CTOD values of type 304 stainless steel pipeline for LNG transmission.

Journal of Mechanical Science and Technology 16 (8): 1064–71. doi:10.1007/bf02984015

Barsom, J. M. & Rolfe, S. T. (1999). *Fracture and Fatigue Control in Structures*. 3rd Editio. Englewood Cliffs, New Jersey: Prentice Hall.

Barsom, J. M & Rolfe, S. T (1970). Correlations Between KIc and Charpy V-Notch Test Results in the Transition-Temperature Range. *Impact Testing of Materials . ASTM STP 466* 1: 281–302.

Beden, S. M., Abdullah, S. & Ariffin, A. K. (2009). Review of Fatigue Crack Propagation Models for Metallic Components. *European Journal of Scientific Research* 28 (3): 364–397.

BS 7910. (2013). Guide to Methods for Assessing the Acceptability of Flaws in Metallic Structures.

Cheng, Y. F. & Xue, H. B. (2011). Characterization of Inclusion of X80 Pipeline Steel and Its Correlation with Hydrogen-Induced Cracking. *Corrosion Science* 53 (4): 1201–1208.

Griffith, A. A. (1920). The Phenomenon of Rupture and Flow in Solids. *Philosophical Transaction, Series A* 221: 163–198.

Hashemi, S. H. (2008). Apportion of Charpy Energy in API 5L Grade X70 Pipeline Steel. *International Journal of Pressure Vessels and Piping* 85: 879–84. doi:http://dx.doi.org/10.1016/ j.ijpvp.2008.04.011.

Hillenbrand, H. G., Liessem, A., Kalwa, C., Erdelen, M. & Stallybrass, M. (2008). Technological Solutions for High Strength Gas Pipelines. http://www.bergpipe.com/files/ep_tp_80_08en.pdf.

Hillenbrand, H. G., Niederhoff, E. Amoris, Perdix, C., Streisselberger, A. & Zeislmair, U. (1999). Development of Linepipe in Grades Up to X100.‖ *Europipe Technical Literature*. Washington.

Omale, J. I. (2016). Micrsotructure and Mechanical Properties of Welds in Pipeline Steel. (Published M.Sc Thesis). University of Saskatchewan.

Ike, T. M. (2018). Investigation on the Mechanical & Microstructural Behaviour of API X70 Steel Weldment in Seawater. (Unpublished masters Thesis). Federal University of Technology Minna, Nigeria.

Ike, T. M., Adedipe, O., Lawal, S. A., Abolarin, M. S. & Olugboji, O. A. (2019). ‒Investigation of the Mechanical and Microstructural Properties of Welded API X70 Pipeline Steel.‖ *ARID Zone Journal of Engineering, Technology & Environment* 15 (2): 342–354.

Inglis, C. E. (1913). Stresses in a Plate due to the Presence of Cracks and Sharp Corners. *Transaction of the Institute of Naval Architects* 55: 219–241.

Kim, S. H., So, Y. S. & Kim, J. G. (2019). Fracture Behavior of Locally Corroded Steel Pipeline in District Heating System Using the Combination of Electrochemistry and Fracture Mechanics. *Metals and Materials International, 26(11), 1671–1678. doi:10.1007/s12540-019-00481-2*

Kirkhope, K. J., Bell, R., Caron, L. & Basu, R. I. (1997). Weld Detail Fatigue Life Improvement Techniques. Ship Structural Committee, USA.

Lancaster, J. (2005). *Engineering Catastrophes Causes and Effects of Major Accidents*. 3rd Editio. Elsevier Ltd.

Godefroid, L. B., Candido, L. C., Toffolo, R. V. & Barbosa, L. H. (2014). Microstructure and mechanical properties of two Api steels for iron ore pipelines. *Materials Research, 17*, 114–120. doi:10.1590/s1516-14392014005000068

Liessem, A. & Hillenbrand, H. G. (2007). Challenges in Linepipe Manufacturing for High Strenght Pipelines. In *16th Biennal Pipeline Research Joint Technical Meeting*, 1–6. Canberra.

Mannucci, G. & Harris, D. (2002). Fracture Properties of API X100 Gas Pipeline Steels. *Europace,* 1-128

Marandet, G. & Sanz, B. (1977). ‒Evaluation of the Toughness of Thick Medium Strength Steels by LEFM and Correlations Between KIc and CVN.‖ In *In ASTM STP631 Flaw Growth and Fracture*, 72–95.

Muneer, B., Ehab, E., Mahmoud, S., Abdulhakim, A., Waleed, A. & Khaled, A. (2015). Mechanical Properties, Microstructure and Toughness Assessment of an X70 Pipeline Steel. *Materials Testing* 57 (10): 897–903. doi.org/10.3139/120.110796

Murakami, Y. (2019). *Metal Fatigue: Effect of Small Defects and Nonmetallic Inclusions*. 2nd Editio. Academic Press. doi:https://doi.org/10.1016/C2016-0-05272-5.

Mustapha, A. (2010). The Effect of Microstructure on the Susceptibility of Pipeline Steels

to Environment-Assisted Cracking. (Published PhD Thesis). Newcastle University, United Kingdom.

Naidu, D., Selahattin, O. & Kevin, M. (2003). *Modeling, Sensing and Control of Gas Metal Arc Welding*. San Francisco, CA: Elsevier Science.

Nonn, A. & Holger, B. (2014). Establishing the Correlation Between Charpy Impact Energies for Different Sized Specimens of Modern Pipeline Steels. In *Proceedings of the 10th International Pipeline Conference*, 1–11. Calgary, Alberta, Canada.

Omale, J. I., Oheri, E. G., Tiamiyu, A. A., Eskandari, M. & Szpunar, J. A. (2017). Microstructure, Texture Evolution and Mechanical Properties of X70 Pipeline Steel after Different Thermo Mechanical Treatments. *Material Science and Engineering* 703: 497–485.

Palmer, A. C. & King, R. A. (2004). *Subsea Pipeline Engineering*. Tulsa, Oklahoma: PennWell Corporation

Pengyan, W., Zheng, L., Zheng, S., Yameng, Q., Wang, J. & Zheng, X. (2015). Tensile and Impact Properties of X70 Pipeline Steel Exposed to Wet H2S Environments. *International Journal of Hydrogen Energy* 13: 1154–1162.

Pilkey, W. D. & Pilkey, D. F. (2008). *Peterson's Stress Concentration Factors*. 3rd Editio. Hoboken, New Jersey: John Wiley and Sons, Inc.

Pipinato, A. (2015). *Innovative Bridge Design Handbook*. Oxford, United Kingdom: Butterworth-Heinemann.

Roberts, R. & Newton, C. (1984). Report on Small-Scale Test Correlations with KIC Data. Weld Research Council Bull.

Rossini, N. S., Dassisti, M., Benyounis, K. Y. & Olabi, A. G. (2012). Methods of Measuring Residual Stresses in Components. *Materials & Design*, 572–88. doi:10.1016/j.matdes.2011.08.022.

Rudawska, A. (2019). *Surface Treatment in Bonding Technology*. San Francisco, CA: Academic press.

Sailors, H. T. & Corten, R. H. (1972). Relationship Between Material Fracture Toughness Using Fracture Mechanics and Transition Temperature Tests. In *National Symposium on Fracture Mechnanics, ASTM STP 514*, 164–191.

Schijve, J. (2009). Fatigue of Structures and Materials. In *Fatigue of Structures and Materials*, Second, 457–79. Dordrecht ; London

Sharma, S. K. & Maheshwari , S. (2017). A Review on Welding of High Strength Oil and Gas Pipeline Steels. *Journal of Natural Gas Science and Engineering* 38, 203–17. doi:10.1016/j.jngse.2016.12.039.

Shifler, D. A. & Denise, M. A (2005). Factors Affecting Corrosion Performance and Testing of Materials and Components in Seawater. In *NACE International Corrosion Conference*, 1–15. Houston, Texas.

Shin, S. Y., Woo, K. J., Hwang, B., Kim, S. & Lee, S. (2009). Fracture-Toughness Analysis in Transition-Temperature Region of Three American Petroleum Institute X70 and X80 Pipeline Steels. *Metallurgical and Materials Transactions A* 40, 867–76. doi:10.1007/s11661-008-9764-2.

Vesga R. W. (2014). Structural Integrity of Steel Pipelines for CO_2 Transport. (Published PhD Thesis). Cranfield University.

Wallin, K., Nevasmaa, P., Laukkanen, A. & Planman, T. (2004). Master Curve Analysis of Inhomogeneous Ferritic Steels. *Engineering Fracture Mechanics* 71 (16): 2329–2346.

Wang, X., Tang, X., Wang, L., Wang, C. & Guo, Z. (2014). Corrosion Behavior of X80 Pipeline Steel under Coupling Effect of Stress and Stray Current. *International Journal of Electrochemical Science*, 4574–4588.

Weman, K. (2003). *Welding Process Handbook*. Abington Cambridge, England: Woodhead Publishing Ltd

Yang, Y., Feng, Liu. & Feng, Xi. (2020). Tensile Fracture Behavior of Corroded Pipeline : Part 1 — Experimental Characterization. *Advances in Material Science and Engineering*. doi:https://doi.org/10.1155/2020/4058452.

Appendix A

Appendix A

Table AI: Calculated fracture toughness values for different authors (parent material)

Temperature (°C)	BS7910 (2013) (MPa√m)	Barsom & Rolfe 1970(1) (MPa√m)	Barsom & Rolfe 1970(2) (MPa√m)	Sailors & Corten 1972 (MPa√m)	Marandet & Sanz 1977 (MPa√m)	Roberts &Newton 1984 (MPa√m)	Barsom & Rolfe 1999 (3) (MPa√m)	Roberts & Newton(2) 1984 (MPa√m)
20	176.92	281.49	123.64	176.17	229.26	195.29	232.23	184.40
10	169.85	265.23	118.84	169.32	220.35	185.77	222.54	171.91
0	164.43	253.01	115.16	164.08	213.53	178.55	215.11	162.07
-10	147.62	216.34	103.74	147.81	192.36	156.55	191.91	129.34
-20	142.46	205.48	100.24	142.83	185.87	149.92	184.74	118.34
-40	126.57	173.20	89.45	127.45	165.86	129.87	162.46	78.66
-60	117.25	155.15	83.12	118.43	154.12	118.40	149.22	44.94
-80	104.08	130.79	74.18	105.69	137.54	102.58	130.19	
-100	94.60	114.14	67.74	96.51	125.60	91.49	116.17	
-120	79.67	89.51	57.60	82.07	106.81	74.59	93.25	
-160	47.77	44.11	35.94	51.20	66.64	41.16	32.20	

Table A II: Calculated fracture toughness values for different authors (weld material)

Temperature (°C)	BS7910 (2013) (MPa√m)	Barsom & Rolfe 1970(1) (MPa√m)	Barsom & Rolfe 1970(2) (MPa√m)	Sailors & Corten 1972 (MPa√m)	Marandet & Sanz 1977 (MPa√m)	Roberts &Newton 1984 (MPa√m)	Barsom & Rolfe 1999 (3) (MPa√m)	Roberts & Newton(2) 1984 (MPa√m)
20	205.83	351.11	143.27	204.14	265.66	235.13	271.53	232.38
10	197.63	330.85	137.71	196.21	255.34	223.67	260.42	219.16
0	180.94	290.86	126.37	180.06	234.32	200.74	237.72	191.33
-10	168.61	262.42	118.00	168.12	218.79	184.11	220.84	169.68
-20	163.28	250.45	114.38	162.97	212.09	177.04	213.54	159.96
-40	154.75	231.67	108.59	154.72	201.35	165.81	201.78	143.72
-60	139.74	199.82	98.39	140.19	182.44	146.44	180.94	112.25
-80	124.30	168.75	87.91	125.25	163.00	127.06	159.25	71.74
-100	109.17	140.05	77.63	110.61	143.95	108.64	137.59	
-120	96.86	118.04	69.27	98.70	128.44	94.11	119.54	
-160	74.98	82.18	54.42	77.53	100.90	69.43	85.71	